**SMAD4 and TGFβ are architects of inverse genetic programs during fate-determination of antiviral memory CD8 T cells.**

Chandiran K. [1], Suarez-Ramirez, J.E.[1], Hu, Y.[2], Jellison, E.R.[1]., Ugur, Z.[1], Low, J.S.[3], McDonald, B.[4] Kaech, S.M.[4], and Cauley L.S.[1].

[1]Department of Immunology, UCONN Health, Farmington, CT. USA.

[2]Department of Microbiology and Immunology, Emory Vaccine Center. Emory University, GA. USA

[3]Department of Immunobiology, Yale University School of Medicine, New Haven, CT, USA

[4]NOMIS Center for Immunobiology and Microbial Pathogenesis, The Salk Institute for Biological Studies, La Jolla, CA, USA

**CORRESPONDENCE:** Further information and requests for resources and reagents should be directed to and will be fulfilled by the Lead Contact, Dr. Linda Cauley (lcauley@uchc.edu).

**Running title**: The role of SMAD4 during formation of memory CD8+ T cells.

**Key words:** Respiratory infection; cytotoxic T lymphocytes, memory CD8 T cells, homing receptors, transcription factors.

**Abstract**

Transforming growth factor β (TGFβ) is a morphogenic protein that augments antiviral immunity by altering the functional properties of pathogen-specific memory CD8 T cells. During infection, TGFβ inhibits formation of effector ($T_{EFF}$) and circulating memory CD8 T cells, while encouraging tissue-resident memory CD8 T cells ($T_{RM}$) to settle in peripheral tissues. SMAD proteins are signaling intermediates that are used by members of the TGF cytokine family to modify gene expression. Using RNA-sequencing we determined that SMAD4 altered the transcriptional profile of antiviral CTLs during respiratory infection. Our data show that SMAD4 and TGFβ use alternate signaling pathways to cooperatively regulate a collection of genes that determine whether pathogen-specific memory CD8 T cells localize in peripheral or lymphoid tissues. During infection, SMAD4 acts independently of TGFβ to inhibit $T_{RM}$ development, while inducing genes that support formation of circulating memory CD8 T cells. The genes that are modulated by SMAD4 include several homing receptors (CD103, KLRG1 and CD62L) and transcription factors (Hobit and EOMES) that support memory formation.

## Introduction

Influenza viruses are highly contagious pathogens that enter the body via the respiratory tract. Cytotoxic T lymphocytes (CTLs) help control these infections by eliminating cells that support the pathogen's lifecycle. Pathogen-specific CTLs differentiate into multiple subsets of effector ($T_{EFF}$) and memory CD8 T cells that perform distinct functions during the immune response. These subsets can be distinguished using homing receptors that support localization in different anatomical niches. Although many studies show that inflammatory mediators have important functions during lineage-specification of pathogen-specific CTLs, the mechanisms that coordinate changes homing receptor expression during infection are poorly understood. Our data show that a network of signaling pathways, that are controlled by members of the transforming growth family (TGF), alter the functional attributes of pathogen-specific CTLs during memory formation.

To augment immunity, pathogen-specific CTLs must distribute to peripheral and lymphoid tissues. A response to infection is initiated by naïve CD8 T cells that migrate through secondary lymphoid organs (SLO). Circulating lymphocytes enter resting lymph nodes from wide blood vessels known as high endothelial venules (HEV) (Mionnet et al., 2011). During transit through HEVs, CD62L interacts with carbohydrates expressed on the surface of activated endothelial cells and initiates an adhesion cascade that results in transendothelial migration (Ding et al., 2000). Inside the lymph node, pathogen-specific CTLs encounter antigen presenting cells (APCs) bearing pathogen-derived peptides and undergo clonal expansion as CD62L is replaced with adhesion molecules that facilitate migration to infected tissues.

Infected host cells produce large quantities of pro-inflammatory cytokines that orchestrate an immune response. Interleukin (IL)-2 and IL-12 promote formation of short-lived $T_{EFF}$ cells that are programmed for an immediate lytic response (Chowdhury et al., 2011). Some $T_{EFF}$ cells express Killer Cell Lectin Like Receptor G1 (KLRG1), which is a membrane-bound adhesion molecule with an immunoreceptor tyrosine-based inhibitory motif (ITIM) in the cytoplasmic tail (Ito et al., 2006; Tessmer et al., 2007). Although most CTLs transiently express KLRG1 during antigen stimulation (Herndler-Brandstetter et al., 2018; Joshi et al., 2007), terminally-differentiated $T_{EFF}$ cells maintain KLRG1 expression and do not convert to a memory phenotype (Dominguez et al., 2015). Most $T_{EFF}$ cells have limited capacity for long-term survival and disappear as the infection resolves, leaving residual populations of memory CD8 T cells in the circulation and peripheral tissues. Central memory

CD8 T cells ($T_{CM}$) enter the bloodstream and transit between secondary lymphoid organs (SLO), whereas peripheral tissues are colonized with tissue-resident memory CD8 T cells ($T_{RM}$) that express CD69 (Mueller et al., 2013). How these different memory subsets augment immunity varies during infections with different types of pathogens. For instance, early recruitment of circulating memory CD8 T cells into the liver is important for control of malaria infection (Lefebvre et al., 2021). Conversely, IAV replicates in the lungs and immunity is facilitated by pulmonary $T_{RM}$ cells that reside near the site of pathogen-exposure (Wu et al., 2014). During respiratory infection, vigorous proliferation by circulating memory CD8 T cells is less desirable, as the lungs may be overwhelmed with massive numbers of $T_{EFF}$ cells (Wu et al., 2014). TGFβ is a suppressive cytokine that can be activated by viral neuraminidase, and dampen the inflammatory response in the lungs during infection with seasonal strains of IAV (Carlson et al., 2010). Continuous exposure to TGFβ is required for $T_{RM}$ cells to express of the cadherin-binding protein αEβ7 integrin (CD103) for enhanced retention in the epithelial layer (Cepek KL et al., 1994; Teraki and Shiohara, 2002).

Cytokines that belong to the TGF family elicit cellular responses via both canonical and non-canonical signaling pathways. Canonical signals are mediated by a cascade of structurally-related molecules known as small (Sma) and mothers against decapentaplegic (Mad)-related (SMAD) proteins (Massagué, 2012). SMAD4 is an adaptor that chaperones phosphorylated receptor-activated SMAD proteins (R-SMADs) into the nucleus to modulate gene expression. We previously used Cre-Lox recombination to determine how signaling via SMAD4 altered the surface markers on antiviral CTLs during IAV infection and found that very few SMAD4-deficient CTLs expressed KLRG1 or CD62L, while abnormal CD103 expression was detected on CTLs in the spleen (Hu et al., 2015). These changes were unexpected, as CTLs displayed a reciprocal phenotype after the TGFβ receptor was ablated (Hu et al., 2015). To further define how SMAD-dependent signaling pathways alter the migratory properties of pathogen-specific CTLs, we have used RNA-sequencing to identify genes that were either induced, or repressed, in the absence of SMAD4. Our data show that a novel SMAD4-dependent signaling pathway alters the expression levels of multiple transcription factors that are known to influence memory formation. Importantly, CD103 expression on $T_{RM}$ cells is induced by a canonical SMAD-dependent signaling pathway during stimulation TGFβ, while an alternative SMAD4-dependent mechanism promotes formation of $T_{EFF}$ and $T_{CM}$ cells in the circulation.

## Materials and methods

### Mice and reagents

Mice were bred and housed at the University of Connecticut Health Center in accordance with institutional guidelines. Experiments were performed in accordance with protocols approved by the UCONN Health Institutional Animal Care and Use Committee (IACUC). Mice that express Cre-recombinase under the control of the distal-Lck promoter (dLck) were used to generate mice that lack R-SMAD2 (S2KO), R-SMAD3 (S3KO), co-SMAD4 (S4KO), EOMES (EKO) and TGFβ receptor II (TR2KO). S4KO and TR2KO were further crossed with OTI mice that express a transgenic antigen receptor specific for the SIINFEKL peptide presented on H-2K$^b$. Virus stocks were grown in fertilized chicken eggs (Charles River) and stored as described previously. Between 8 to 20 weeks (wks) after birth, anesthetized mice were infected intranasally (i.n.) with either 2x10$^3$ plaque-forming units (PFU) X31-OVA, or 5x10$^3$ colony-forming units (CFU) of recombinant *Listeria monocytogenes* expressing chicken ovalbumin (LM-OVA).

### Adoptive cell transfer and sample preparation for flow cytometry

Naïve CD8 T cells were isolated from SLO using Mojosort isolation kits (Biolegend, Dedham MA). Mice received 5x10$^3$ congenically-marked donor cells by intravenous (i.v.) injection given 48 hours (hrs) before infection. To isolate CTLs for flow cytometry, chopped lung tissue was incubated at 37°C for 90 minutes (mins) in RPMI with 5% fetal bovine serum (FBS) and 150 U/ml collagenase (Life Technologies, Rockville, MD, USA). Nonadherent cells were enriched on Percoll density gradients (44/67%) spun at 1200*g* for 20 min. Lymphocytes were incubated with antibodies that block Fc-receptors (15 mins at RT). Antigen-experienced CD8 T cells were identified using high CD11a/CD44 expression and divided into subsets with antibodies specific for CD103, KLRG1, CD127 and CD62L. For intracellular staining, lymphocytes were analyzed using True Nuclear transcription factor buffer (Biolegend, Dedham-MA). Permeabilized cells were stained with antibodies specific for T-bet and EOMES. Stained cells were collected using a BD LSRII with FACSDiva V8.0 (BD Biosciences) and subsequently analyzed using Flowjo® and Graphpad Prism software.

For imaging flow cytometry, cells were treated as above and permeabilized using 90% ice cold methanol for intracellular staining. Cells were imaged using an Amnis ImagestreamX MKII flow cytometer with an 40x objective and analyzed with Amnis Ideas V6.2 (Luminex) software.

**Cell culture**

Naïve CD8 T cells were grown in RPMI with 10% FBS, L-glutamine, β-mercapthoethanol, sodium pyruvate, HEPES, and antibiotics. For T cell receptor (TcR) stimulation, CTLs were stimulated with plate-bound anti-CD3/CD28 (1μg/ml) and rIL-2 (20 U/ml). After 48hrs, CTLs were transferred to new wells for cytokine stimulation without TcR stimulation. Replicate wells were supplemented with rIL-2 (20 U/ml), ALK5 inhibitor (SB431542, 10μM/ml), and TGFβ (10 ng/ml).

**RNA-sequencing and gene set enrichment analysis.**

Messenger-RNA was extracted from purified CTLs using RNAeasy Plus Mini Kits (Qiagen, Hilden Germany) and sequenced by Otogenetics Corporation (Atlanta, GA). RNA-sequences from OTI-S4KO and OTI-Ctrl cells are available in the GEO database (accession # GSE151637). Data were analyzed using Tophat2, Cufflinks and Cuffdiff software (DNAnexus, Mountain View, CA). Transcriptional changes greater than two-fold (Log2 fold change >1 or <-1, $p<0.05$, false discovery rate<0.05) were used to select genes for Ingenuity pathway (Qiagen, Hilden Germany) and gene set enrichment analysis (GSEA) (Broad Institute, San Diego CA)(Subramanian et al., 2005). Differentially expressed genes were compared with published datasets, using GEO accession #s GSE39152(Wakim et al., 2012), GSE107281(Milner et al., 2017), GSE70813(Mackay et al., 2016), and GSE125471(Nath et al., 2019). Normalized enrichment scores (NES) and false discovery rates (FDR) were calculated using ggplot2 package in R.

**Retroviral transduction**

A murine stem cell virus (MSCV)-IRES-GFP (pMig)-EOMES vector (RV-EOMES-GFP) was used for ectopic gene expression in activated CD8 T cells(Pearce et al., 2003). Viruses were packaged in human embryonic kidney (HEK) 293 cells and viral supernatants were processed using Retro-X concentrators (Takara Bio. USA Inc). Naïve CD8 T cells were purified by negative-selection and stimulated *in vitro* with plate-bound anti-

CD3/CD28. After 48hrs, activated CD8 T cells were spin-infected (1800*g*, 60 min, 30$^{o}$C) using concentrated supernatants and polybrene (1 µg/ml). After 3hrs, the washed cells were cultured in complete RPMI.

**Statistical analysis**

P values were calculated using two-way ANOVA followed by Tukey's multiple comparison tests. Horizontal lines indicate comparisons between samples.

**Results**.

*SMAD4 alters homing receptor expression in the absence of TGFβ.*

We previously used genetically-modified mice to compare surface markers that were expressed on antiviral CTLs that lacked either SMAD4 (S4KO), or TGFβ receptor II (TR2KO). Both mutations altered the expression levels of several homing receptors that identify specialized memory CD8 T cells (Hu et al., 2015). Since SMAD4 is an adaptor for multiple signaling pathways within the SMAD cascade, we interbred S4KO and TR2KO mice to produce CTLs that lack both signaling intermediates (S4TR2-DKO). The mice were further crossed with OTI mice that expressed a transgenic antigen-receptor that is specific for a peptide (SIINFEKL) derived from chicken ovalbumin (OVA) presented on H-2K$^b$ (Hogquist et al., 1994). To compare surface antigens during IAV infection, we transferred naïve donor cells from OTI-TR2KO, OTI-S4KO and OTI-S4TR2-DKO mice to C57BL/6 mice before infection with X31-OVA. Cre-deficient littermates (OTI-Ctrl) were used as controls. On different days post infection (dpi), donor cells in the lungs and spleens were analyzed by flow cytometry **(Fig. 1A)**.  The heat map show percentages of donor cells that expressed CD103, KLRG1, CD62L and CD127.

KLRG1, CD62L and CD127 (IL-7 receptor) are surface markers that can distinguish short-lived $T_{EFF}$ cells (SLEC) from memory precursors (MPECS), while CD103 is expressed on large numbers of $T_{RM}$ cells in peripheral tissues (Joshi et al., 2007; Mueller et al., 2013). CD103 and KLRG1 are cadherin-binding proteins that interact with stromal cells during cell-migration and cytolysis (Ito et al., 2006; Karecla et al., 1995). $T_{RM}$ cells only express CD103 during chronic stimulation with TGFβ, while this cytokine inhibits formation $T_{EFF}$ cells that express KLRG1 (Sanjabi et al., 2009; Teraki and Shiohara, 2002). Consistently, large numbers of OTI-TR2KO cells expressed KLRG1 in the lungs, while CD103 was absent. As the infection progressed, CD62L reappeared on OTI-Ctrl cells and OTI-TR2KO cells in the spleens, indicating conversion to a $T_{CM}$ phenotype. Consistent with our previous report, very few OTI-S4KO cells expressed KLRG1 or CD62L, while CD103 was expressed on CTLs in the spleen (Hu et al., 2015). Since OTI-S4KO and OTI-S4TR2-DKO cells displayed similar phenotypes at all time points analyzed **(Fig 1A)**, these data indicate that SMAD4 alters the expression levels of multiple homing receptors via a TGFβ independent pathway.

*In vitro* naïve CD8 T cells downregulate CD103 during TcR stimulation. We previously found that although newly activated CTLs re-expressed CD103 during stimulation with TGFβ, this marker was not induced on $T_{CM}$ cells during stimulation under similar conditions (Mani et al., 2019; Suarez-Ramirez et al., 2019). In agreement with these studies, we found that similar percentages of naïve CD8 T cells from each group of donor mice expressed CD103 before transfer, whereas this marker was mostly absent at 6dpi. As the infection progressed, 30% of OTI-Ctrl cells re-expressed CD103 in the lungs but not the spleen, indicating a response to TGFβ **(Fig. 1B)**. Although OTI-S4KO and OTI-S4TR2-DKO cells lacked CD103 expression after antigen stimulation, this marker was re-expressed with accelerated kinetics and maintained in both tissues throughout the time period studied.

Rodents lose large percentages of their body weight during IAV infection and the rate of recovery to normal size can be used to evaluate the severity of disease. We previously showed that S4KO mice lost more weight and recovered from IAV infection more slowly than littermate controls (Hu et al., 2015). Since OTI-S4KO and OTI-S4TR2-DKO cells displayed very similar phenotypes during IAV infection, we infected S4TR2-DKO and S4TR2-Ctrl mice with X31-OVA (H3N2 serotype) to monitor disease progression **(Figure Supplement 1A).** Changes in body weight are shown as percentages of the starting value. The S4TR2-DKO mice that lost more weight and recovered from infection more slowly than the control mice. After 30 days, the immune mice were challenged with a serologically distinct strain of IAV (WSN-$OVA_I$ H1N1 serotype) to assess heterosubtypic immunity provided by antiviral CTLs **(Figure Supplement 1B)**. Unprimed mice were used as a positive control for weight loss. Since the two groups of immune mice did not experience substantial weight loss during infection with WSN-$OVA_I$, our data indicate that protection against reinfection was not dependent on SMAD4 or TGFβ.

*The transcriptional profile of SMAD4-deficient CTLs is similar to $T_{RM}$ cells*.

Although gene regulation by TGFβ has been analyzed in considerable detail, little is known about the function of SMAD4 during functional specialization of antiviral CTLs. To reveal how SMAD4 alters homing receptor expression on antiviral CTLs, we used RNA-sequencing to compare differentially expressed genes in SMAD4-deficient and control CTLs. Naïve OTI-S4KO and OTI-S4Ctrl cells were transferred to C57BL/6 mice before infection with X31-OVA. Early effector (EE) cells are defined as activated CTLs that have not committed to

SLEC/MPEC phenotypes. To analyze phenotypically similar populations of antigen-specific CTLs, EE cells were isolated from the spleens at 6dpi, using CD45.1$^{+}$CD44$^{+}$, KLRG1$^{-}$, CD127$^{-}$, CD103$^{-}$. Samples were analyzed in triplicate and RNA-sequences were registered with the GEO repository (Accession # GSE151637). A comparison of the transcripts that were expressed in OTI-S4KO and OTI-Ctrl cells revealed many differentially-expressed genes **(Fig. 2A)**. Notably, EOMES (*Eomes*) and CD62L (*Sell*) were expressed at reduced levels in OTI-S4KO cells, while *Itgae* (encodes a subunit of CD103) expression increased **(Fig. 2B)**. As large numbers of mucosal $T_{RM}$ cells express CD103, we used gene set enrichment analysis (GSEA) to compare the transcriptional profile of OTI-S4KO cells with the signature genes expressed in $T_{RM}$ cells from other tissues **(Fig 2C).** Similarities between the datasets revealed a strong correlation between the transcriptional profile of OTI-S4KO cells and genes expressed in $T_{RM}$ cells recovered from the gastrointestinal tract, brain, liver, as well as CTLs that were stimulated with TGFβ *in vitro* (Mackay et al., 2016; Milner et al., 2017; Nath et al., 2019; Wakim et al., 2012) **(Fig. 2D)**. These consistent profiles indicate that early signaling via SMAD4 impedes differentiation towards a 'resident memory' phenotype, that is normally associated with stimulation by TGFβ.

*SMAD4 modifies the transcriptional program of developing memory CD8 T cells.*

The signals that determine whether CTLs differentiate into $T_{CM}$ or $T_{RM}$ cells are poorly defined, however several transcription factors have been implicated in this process. These molecules include Hobit, which is expressed during $T_{RM}$ differentiation (Mackay et al., 2016; Parga-Vidal et al., 2021) and EOMES which is associated with formation of $T_{CM}$ cells (Intlekofer et al., 2005). RNA-sequencing showed that OTI-S4KO cells produced fewer *Eomes* transcripts than control cells in during IAV infection **(Fig 2B)**. We next activated S4KO cells *in vitro* with anti-CD3/28 for 48hrs, followed by stimulation with rIL-2 for 48hrs without TcR activation. Some wells were supplemented with an ALK 5 inhibitor to prevent a response to TGFβ that was present in the media. qPCR analysis showed that the S4KO cells produced more Hobit transcripts than S4Ctrl cells during culture with rIL-2 **(Fig 2E).** Importantly, Hobit expression in S4Ctrl cells decreased when the ALK 5 inhibitor was present, while expression in S4KO cells did not change.

Prior studies show that EOMES is expressed in $T_{CM}$ cells and repressed by TGFβ during formation of $T_{RM}$ cells (Mackay et al., 2015; Skon et al., 2013). The peripheral tissues of EOMES-deficient mice contained

expanded populations of $T_{RM}$ cells after LCMV infection, while EOMES expression in wildtype CTLs was inversely correlated with Hobit (Parga-Vidal et al., 2021). Since EOMES has an important function during memory formation, we used intracellular staining to verify that EOMES expression in antiviral CTLs was altered in the absence of SMAD4.

Naïve OTI-S4KO and OTI-S4Ctrl cells were transferred to C57BL/6 mice before infection with X31-OVA. OTI-TR2KO and OTI-TR2Ctrl cells were used for comparison. On different days after infection, intracellular staining was used to compare T-bet and EOMES expression by conventional **(Fig. 2F)** and imaging flow cytometry **(Fig. 2H-J)**. Similar to prior reports, OTI-TR2KO cells expressed EOMES at higher levels than control cells. Conversely, OTI-S4KO cells expressed EOMES at lower levels than control cells in the lungs and a similar trend was observed in the spleens **(Fig. 2F)**. These data indicate that EOMES is repressed by TGFβ during $T_{RM}$ formation, while an alternative SMAD4-dependent mechanism induces EOMES expression in $T_{CM}$ cells. We used imaging flow cytometry to compare nuclear localization of EOMES in the donor cells at 8dpi **(Fig. 2H-J).** The data show that EOMES was not only expressed at reduced levels in S4KO cells, but a smaller percentage of protein was located in the nucleus, where it could influence T cell differentiation. These changes in EOMES expression are consistent with the idea that S4KO cells are predisposed to become $T_{RM}$ cells, rather than $T_{CM}$ cells. SMAD4-ablation caused minor changes in T-bet expression **(Fig 2G)**.

Prior studies show that viral neuraminidase activates TGFβ and dampens the inflammatory response in the lungs during IAV infection (Schultz-Cherry and Hinshaw, 1996). To avoid the influence of virus-activated TGFβ, we performed similar experiments with mice that were infected with recombinant *Listeria monocytogenes* (LM) encoding chicken ovalbumin (LM-OVA) (Pope et al., 2001). This intracellular bacterium is known to induce a systemic inflammatory response that promotes formation of $T_{EFF}$ cells that express KLRG1 (Obar et al., 2011). The experiments confirmed that TGFβ and SMAD4 modify EOMES expression in opposite directions during infection with LM-OVA **(Figure Supplement 2A and 2B)**. We next used qPCR analysis to determine whether OTI-S4KO cells produced *Klrg1* transcripts during infection with LM-OVA. OTI-S4KO and OTI-Ctrl cells were sorted from the spleens at 8dpi, using CD45.1 expression. The experiment showed that OTI-S4KO cells produced fewer *Klrg1* transcripts than OTI-S4Ctrl cells **(Figure Supplement 3)**. Although KLRG1 was expressed on large numbers of OTI-TRKO cells during infection with LM-OVA, this marker was

not expressed on OTI-TRKO cells during culture with rIL-12 *in vitro* (data not shown), indicating a requirement for additional stimuli. These experiments show that TGFβ and SMAD4 cooperatively regulate a collection of genes that support memory formation. Importantly, SMAD4 can alter gene expression independently of TGFβ.

*SMAD4 and TGFβ induce reciprocal changes in gene expression*.

In wildtype animals, continuous signaling via the TGFβ receptor is required for $T_{RM}$ cells to maintain CD103 expression (Zhang and Bevan, 2013). *In vivo*, some naïve CD8 T cells are preconditioned to become $T_{RM}$ during interactions with antigen presenting cells (APCs) that activate TGFβ in the lymph nodes (Mani et al., 2019). Since immune cells produce large quantities of pro-inflammatory molecules during infection, we used *in vitro* stimulation to further explore how newly activated CTLs respond to stimulation with TGFβ.

Naïve CD8 T cells were isolated from SLO by negative-selection and activated with plate-bound anti-CD3/CD28 plus recombinant IL-2 (20u/ml), to mimic antigen stimulation. The remaining CTLs were washed and cultured in fresh media without TcR stimulation. Replicate wells were supplemented with either rIL-2 alone, or rIL-2 plus exogenous TGFβ (10ng/ml). RNA was extracted at 24hrs and 48hrs after cytokine stimulation (i.e. 72hrs and 96hrs after TcR stimulation, respectively) for qPCR analysis **(Fig. 3A)**. The graphs show relative changes in gene expression ($log_2$ fold change) compared to the controls.

RNA was extracted from S4Ctrl cells at 48hrs after TcR stimulation for use as a reference sample. These cells contained very few *Itgae* transcripts. After stimulation with rIL-2, S4Ctrl cells showed a modest increase (3-fold) *Itgae* expression, indicating that the cultures contained some autocrine or media-derived TGFβ, as CD103 expression is TGFβ-dependent. As expected, the numbers of *Itgae* transcripts increased (6-fold) when S4Ctrl cells were treated with exogenous TGFβ **(Fig3A)**. During IAV infection, S4KO cells expressed CD103 at higher levels than S4Ctrl cells **(Fig 1B)**. Consistently, S4KO cells produced more *Itgae* transcripts than S4Ctrl cells during culture with rIL-2 alone. The numbers of *Itgae* transcripts increased when S4KO cells were treated with exogenous TGFβ, indicating normal signal transduction by the TGFβ receptor.

Ex-vivo analysis showed OTI-S4KO cells expressed EOMES at reduced levels during IAV infection **(Fig 2)**. To further explore how this transcription factor was regulated, we used qPCR to analyzed *Eomes* transcripts in CTLs after cytokine stimulation *in vitro* **(Fig. 3B)**. Naïve S4Ctrl and S4KO cells were activated

with anti-CD3/CD28 (48hrs) and stimulated with cytokines as previously. RNA was extracted from S4Ctrl cells at 48hrs after TcR stimulation to provide a reference sample. The experiment showed a transient reduction in the numbers of *Eomes* transcripts in S4Ctrl cells during culture with rIL-2, while expression returned to baseline at 96hrs after TcR stimulation. As expected, *Eomes* expression decreased when S4Ctrl cells were stimulated with TGFβ. The S4KO cells also expressed *Eomes* transcripts at low levels during culture with rIL-2, however expression continued declining until 96hrs after TcR stimulation and was not altered by the addition of TGFβ. These data show that EOMES is downregulated by TGFβ, while a second SMAD4-dependent signaling pathway is required for antigen-experienced CTLs to maintain EOMES expression during culture with IL-2.

*TGFβ can induce CD103 expression on CTLs independently of SMAD4.*

Prior studies show considerable redundancy within the SMAD signaling cascade. Notably, R-SMAD2 and R-SMAD3 heterodimers entered the nucleus of cancer cells without SMAD4 (Fink et al., 2003). To further define how TGFβ induces CD103 expression, we produced CTLs that lacked either R-SMAD2 (S2KO), or R-SMAD3 (S3KO) and both molecules (S23-DKO). The S3KO were also crossed with S4KO mice to produce CTLs that lacked both R-SMAD3 and co-SMAD4 (S34-DKO). The respective Cre-deficient littermates were used as controls.

To analyze CD103 expression, naïve CD8 T cells were activated *in vitro* for 48hrs before stimulation with TGFβ as above. The cultured cells were analyzed by flow cytometry at 96hrs after TcR stimulation **(Fig 3C)**. As expected, wildtype CTLs expressed CD103 during stimulation with TGFβ and the pattern did not change in the absence of R-SMAD2, or R-SMAD3. Conversely, S23-DKO, or TR2KO cells did not express CD103 under any conditions analyzed. When we analyzed CD103 expression in the absence of SMAD4, we found that S4KO, S34KO and S4TR2-DKO cells all expressed CD103 at intermediate levels during stimulation with rIL-2. CD103 expression increased when S4KO cells were stimulated with TGFβ, while expression on S34KO and S4TR2-DKO cells did not change. We compared the nuclear localization of R-SMAD2/3 in OTI-S4KO and OTI-S4Ctrl cells at 8dpi with X31-OVA **(Fig 3D-E).** Imaging flow cytometry showed no difference between the distributions of R-SMAD2/3 in the two donor populations. Together, these data show that SMAD4 has multiple functions during regulation of CD103. During stimulation with TGFβ, R-SMAD3 combines with either R-SMAD2 or

SMAD4 to induce CD103 expression. Since SMAD4 was not required for canonical TGFβ signaling, the phenotypic changes in SMAD4-deficient CTLs could not be attributed to dysregulated a feedback mechanism.

*SMAD4 and EOMES prevent CD103 expression on antigen-experienced CTLs.*

Two mechanisms that repress *Itgae* gene have been described previously. Ski is a nuclear proto-oncogene that inhibits TGFβ signaling through interactions with SMAD proteins (Sun et al., 1999). In activated CTLs, CD103 can be repressed by Ski/SMAD4 heterodimers that bind to a regulatory sequence in the *Itgae* gene (Wu et al., 2020). However, there is currently no evidence that Ski alters CD62L or KLRG1 expression. Others found evidence that CD103 was down-regulated by EOMES during formation of $T_{RM}$ cells (Mackay 2015). Since we found that SMAD4-deficient CTLs expressed EOMES at reduced levels during IAV infection, we reasoned that SMAD4 might indirectly alter *Itgae* expression through EOMES induction. To explore this possibility, we intercrossed S4KO and EOMES-deficient (EKO) mice to produce CTLs with both mutations (ES4KO). The respective Cre-deficient littermates (ECtrl, S4Ctrl and ES4Ctrl) were used as controls. Naïve CD8 T cells were activated *in vitro* (48hrs) and stimulated with cytokines (48hrs) as previously. Selected wells were supplemented with an ALK5 inhibitor (SB431542) throughout the experiment to prevent signaling via the TGFβ receptor. At 96hrs after TcR stimulation, CTLs were analyzed for CD103 expression by flow cytometry **(Fig. 4A)**. Although the control cells did not express CD103 during culture with IL-2, this marker was induced by TGFβ. The S4KO and EKO cells both expressed CD103 at intermediate levels during culture with rIL-2 and expression increased when TGFβ was added. Conversely, ES4KO cells expressed CD103 at high levels under all conditions analyzed and did not change when TGFβ was used.

To further explore whether EOMES altered the phenotype of S4KO cells, we used the (MSCV)-IRES-GFP (pMIG) retroviral vector to over-express EOMES (plus GFP) in antigen-experienced CTLs *in vitro* (**Fig.4B**). The pMIG vector has been described previously (Pearce et al., 2003). Naïve S4KO and EKO cells were stimulated with anti-CD3/28 and rIL-2 (48hrs), then transduced with either EOMES-IRES-GFP, or empty vector control (EV-IRES-GFP). At 96hrs after TcR stimulation, the $GFP^+$ CTLs were analyzed for CD103 expression by flow cytometry. Eomes expression in EKO cells was used to verify that the RV-EOMES-GFP vector was functional (overlaid histograms) (**Fig.4B**). After EOMES was over-expressed, smaller percentages of S4KO and S4Ctrl

cells expressed CD103 **(Fig. 4C)**. Since the phenotype of S4KO cells was partially restored after EOMES transduction, these data are consistent with repression of the *Itgae* gene by multiple mechanisms. These mechanisms include interactions with Ski/SMAD4 heterodimers (Wu et al., 2020), as well as via EOMES induction.

*SMAD4 is required for Sell expression in $T_{CM}$ cells.*

L-selectin (CD62L) is the principal marker used to identify $T_{CM}$ cells (Sallusto et al., 1999). Small numbers of OTI-S4KO cells expressed CD62L after infection X31-OVA **(Fig. 1A)**, indicating a defect during formation of circulating memory CD8 T cells. To determine whether the defect was due to a reduction in EOMES expression, we infected S4KO, EKO, and ES4KO mice (plus littermate controls) with X31-OVA. At 30dpi, different tissues were analyzed for OVA-specific CTLs using MHCI tetramers. Anti-CD8 antibodies were administered to the mice by i.v. injection 3 mins before sacrifice to stain CTLs in the bloodstream. Before infection, CD62L was expressed at similar levels on CD8 T cells from each group mice **(Fig. 5A).** At 30dpi, CD62L was expressed on ~50% OVA-specific CTLs in the ILN from the control mice, indicating the presence of $T_{CM}$ cells. Smaller percentages of OVA-specific CTLs expressed CD62L in the ILNs from S4KO and ES4KO mice (17-22%), supporting the idea that signaling via SMAD4 promotes formation of $T_{CM}$ cells **(Fig. 5B)**. As expected, the lungs and draining lymph nodes (dLN) from each group of mice contained $CD103^+$ $T_{RM}$ cells. In addition, abnormal CD103 was expression was detected on OVA-specific CTLs in the spleens from S4KO and ES4KO mice

Kruppel-like factor 2 (KLF2) is a zinc-finger transcription factor that is required to induce *Sell* expression, and can be down-regulated by TGFβ during $T_{RM}$ formation (Bai et al., 2007; Skon et al., 2013). We used qPCR analysis to determine whether SMAD4 was required for antigen-experienced CTLs to re-express the *Sell* gene **(Fig 5C)**. S4KO and S4Ctrl cells were activated *in vitro* (48hrs) and stimulated with rIL-2 (48hrs), as previously. mRNA was extracted from S4Ctrl cells at 48hrs after TcR stimulation for a reference sample. The experiments showed that S4KO cells produced fewer *Sell* transcripts than control cells during stimulation with rIL-2, while *Klf2* was expressed at similar levels. These data indicate that SMAD4 acts independently of KLF2 to induce CD62L expression in circulating memory CD8 T cells.

Prior studies indicate that EOMES is required for formation $T_{CM}$ cells (McLane et al., 2013) and down-regulated by TGFβ as $T_{RM}$ cells settle in peripheral tissues (Mackay et al., 2015). Since S4KO cells expressed EOMES at reduced levels in during IAV infection **(Fig 2)**, we reasoned that SMAD4 might indirectly increase *Sell* expression by inducing EOMES. To explore this possibility, we activated S4KO, EKO and ES4KO cells (plus Cre-deficient controls) *in vitro,* using plate-bound antibodies as previously. Selected wells were supplemented with SB431542 throughout the experiment, to prevent TGFβ signaling. Naïve CD8 T cells from each group of mice expressed CD62L at similar levels before culture (**Fig. 5B**). Naïve CD8 T cells were activated with antibodies (48hrs) and stimulated cytokines (48hrs) as previously (**Fig. 5D**). The control cells down-regulated CD62L during TcR stimulation and expression returned during culture with rIL-2 **(Figure Supplement 4)**. Approximately 80% of control cells re-expressed CD62L in the cultures that contained ALK5 inhibitor (SB431542), and expression declined to 25% during culture with IL-2 and TGFβ. Only 50% of S4KO and ES4KO cells expressed CD62L during culture with rIL-2/SB431542 and thus number did not change when TGFβ was present. These data indicate that newly activated CTLs down-regulate CD62L during stimulation TGFβ, while SMAD4 is required for CTLs to re-express CD62L after antigen-stimulation.

To explore whether EOMES was required for antigen-experienced CTLs to re-express CD62L during memory formation, we used the EOMES-IRES-GFP retroviral vector to over-express EOMES in S4Ctrl and S4KO cells, as described previously. Naïve CD8 T cells were activated *in vitro* and transduced with EOMES-IRES-GFP or EV-IRES-GFP vectors. At 96hrs after TcR stimulation, $GFP^+$ cells were analyzed for CD103 and CD62L expression. Transduction with the EOMES-IRES-GFP vector induced reciprocal changes in the percentages of S4Ctrl cells that expressed CD103 and CD62L (**Fig. 5E**), thus indicating a shift toward a 'central memory' phenotype. The changes in CD62L expression were less pronounced in S4KO cells, than the control cells, indicating that additional stimuli were required to induce *Sell* expression.

To explore whether TGFβ down-regulates CD62L via a canonical signaling pathway we activated S2KO, S3KO, S23-DKO and S4KO cells *in vitro* as previously. Selected wells were supplemented with SB431542 throughout the experiment. At 48hrs after cytokine stimulation, CTLs were analyzed by flow cytometry **(Fig. 5F)**. Approximately 80% control cells expressed CD62L after culture with rIL-2 plus SB431542, while expression decreased in the presence of TGFβ. This pattern was not altered in the absence of either R-

SMAD2 (S2KO) or R-SMAD3 (S3KO). Conversely, CD62L was expressed on 50% of S4KO, S34-DKO and S4TR2-DKO cells during culture with IL-2/SB431542, while TGFβ had no effect. These data indicate that TGFβ represses the *Sell* gene via a canonical R-SMAD2/3 dependent pathway. Conversely, SMAD4 acts independently of TGFβ to induce *Eomes* and *Sell* expression during formation of $T_{CM}$ cells.

## Discussion

Memory CD8 T cells can be divided into multiple subsets of based on their function, lifespan, and tissue localization. Cells in peripheral and lymphoid tissues express different combinations of homing-receptors, that are induced by integrated signals from the antigen receptor and costimulatory molecules, as well as cytokines that are released during infection. We previously showed that antiviral CTLs express several homing receptors that are regulated via SMAD4, including KLRG1, CD103 and CD62L. To further define how changes in homing receptor expression are coordinated as CTLs respond to infection, we used RNA-seq to compare gene expression in OTI-S4KO and OTI-Ctrl cells during IAV infection. The experiment revealed a pattern of differentially-expressed genes that resembled the transcriptional profile of $T_{RM}$ cells in other non-lymphoid tissues. Genes that are normally associated with formation of $T_{EFF}$ cells and $T_{CM}$ cells were expressed at reduced levels in OTI-S4KO cells, including Eomes, CD62L (*Sell*), and KLRG1 (*Klrg1*). Conversely, OTI-S4KO cells expressed several genes that are normally associated with $T_{RM}$ cells at increased levels including αE integrin (*Itgae*) and Hobit. Our data indicate that SMAD4 and TGFβ perform reciprocal functions during memory formation, as SMAD4 favors formation of circulating memory CD8 T cells and inhibits $T_{RM}$ development, whereas TGFβ inhibits $T_{EFF}$ formation and induces $T_{RM}$ cells.

TGFβ is a pleiotropic cytokine with anti-inflammatory properties and uses a network of interconnected signaling pathways to modulate gene expression. The canonical signaling pathway for TGFβ involves formation of R-SMAD2/3 heterodimers that enter the nucleus with together SMAD4 (ref). Experiments with genetically-modified cells reveal extensive redundance within the SMAD signaling cascade. In cancer cells, R-SMAD2/3 heterodimers entered the nucleus without SMAD4 and changed gene expression (David et al., 2016; Fink et al., 2003; Levy and Hill, 2005). When SMAD4 is present, homodimers that are comprised of either R-SMAD2 or R-SMAD3 are sufficient for signaling transduction (Yagi et al., 1999). Since R-SMAD2 lacks a DNA-binding domain (Yagi et al., 1999), R-SMAD2 homodimers did not alter gene expression in macrophages or helper T cells during stimulation with TGFβ (Chung et al., 2012; Malhotra et al., 2010; Takimoto et al., 2010; Wang et al., 2013). Similarly, R-SMAD2 was not sufficient for TGFβ to induce CD103 expression on CTLs in the absence of either R-SMAD3 and SMAD4.

SMAD proteins modulate gene expression through interactions with numerous transcription factors. In CD8 T cells, SMAD4 forms complexes with a tumor repressor called Sloan Kettering Institute (Ski) protein and directly repressed the *Itgae* gene (Wu et al., 2020). Consistently, we found that exogenous TGFβ was not required for S4KO cells to express CD103 at intermediate levels after antigen stimulation. Others used retroviral vectors to ectopically express T-box transcription factors in activated CTLs during HSV infection and found reduced numbers of $T_{RM}$ cells in the skin when EOMES and T-bet were expressed at high levels (Mackay et al., 2015). Further evidence that these transcription factors interfere with formation of $T_{RM}$ cells includes the observation that reduced EOMES and T-bet expression facilitate $T_{RM}$ development (Laidlaw et al., 2014). To further understand how these transcription factors support memory formation, we investigated whether EOMES was regulated via SMAD4. Our experiments confirmed that EOMES was downregulated by TGFβ acting in combination with R-SMAD2/3. Conversely, we found that SMAD4 was required to maintain EOMES expression in activated CTLs. These experiments indicate that SMAD4 has multiple functions during regulation of CD103, as SMAD4/Ski heterodimers interact with regulatory sequences in the *Itgae* gene (Wu et al., 2020), while SMAD4 indirectly represses CD103 through EOMES induction. The influence of both mechanisms during CTL activation was evidenced by cumulative changes in CD103 expression in the absence of SMAD4 and EOMES **(Fig 4)**.

T-box transcription factors have important functions during differentiation of both $CD4^+$ and $CD8^+$ T cells. For this study, we prevented gene expression in peripheral T cells using Cre expressed under the control of the distal Lck promoter. Although SMAD4-ablation caused extensive phenotypic changes in antiviral CTLs, the surface markers on CD4 T cells were largely unaltered (data not shown). Since CD8 T cells express EOMES at higher levels than CD4 T cells (Zhu et al., 2010), our data are consistent with the view that different mechanisms drive effector and memory formation in the CD8+ and CD4+ lineages.

Many transcription factors have important functions during CD8 T cell differentiation. The major players include Zeb1 and Zeb2, which are homologous proteins that serve opposing functions during memory formation and are inversely regulated by TGFβ. *Zeb1* expression increases in maturing memory $CD8^+$ T cells during exposure to TGF-β, whereas *Zeb2* is down-regulated (Dominguez et al., 2015; Guan et al., 2018). Other studies indicate that DNA-binding inhibitors Id2 and Id3 also have reciprocal functions during fate

determination of activated CTLs (Ji et al., 2011; Omilusik et al., 2018; Yang et al., 2011). Whether SMAD4 alters the expression levels of these transcription factors, or other epigenetic-regulators, during CD8 T cell differentiation needs to be further investigated.

## References


Bai, A., Hu, H., Yeung, M., and Chen, J. (2007). Krüppel-Like Factor 2 Controls T Cell Trafficking by Activating L-Selectin (CD62L) and Sphingosine-1-Phosphate Receptor 1 Transcription. J Immunol *178*, 7632–7639.

Carlson, C.M., Turpin, E.A., Moser, L.A., O'Brien, K.B., Cline, T.D., Jones, J.C., Tumpey, T.M., Katz, J.M., Kelley, L.A., Gauldie, J., et al. (2010). Transforming Growth Factor-β: Activation by Neuraminidase and Role in Highly Pathogenic H5N1 Influenza Pathogenesis. PLoS Pathog *6*, e1001136.

Cepek KL, Shaw SK, Parker CM, Russell GJ, Morrow JS, Rimm DL, and Brenner, M.B. (1994). Adhesion between epithelial cells and T lymphocytes mediated by E-cadherin and the αEβ7 integrin. Nature *372*, 190–193.

Chowdhury, F.Z., Ramos, H.J., Davis, L.S., Forman, J., and Farrar, J.D. (2011). IL-12 selectively programs effector pathways that are stably expressed in human CD8+ effector memory T cells in vivo. Blood *118*, 3890–3900.

Chung, S.W., Kwon, M.-Y., Kang, Y.-H., Chung, H.-T., Lee, S.-J., Kim, H.P., and Perrella, M.A. (2012). Transforming growth factor-β1 suppression of endotoxin-induced heme oxygenase-1 in macrophages involves activation of Smad2 and downregulation of Ets-2. J. Cell. Physiol. *227*, 351–360.

David, C.J., Huang, Y.-H., Chen, M., Su, J., Zou, Y., Bardeesy, N., Iacobuzio-Donahue, C.A., and Massagué, J. (2016). TGF-β Tumor Suppression through a Lethal EMT. Cell *164*, 1015–1030.

Ding, Z., Xiong, K., and Issekutz, T.B. (2000). Regulation of chemokine-induced transendothelial migration of T lymphocytes by endothelial activation: differential effects on naive and memory T cells. J Leukoc Biol *67*, 825–833.

Dominguez, C.X., Amezquita, R.A., Guan, T., Marshall, H.D., Joshi, N.S., Kleinstein, S.H., and Kaech, S.M. (2015). The transcription factors ZEB2 and T-bet cooperate to program cytotoxic T cell terminal differentiation in response to LCMV viral infection. Journal of Experimental Medicine *212*, 2041–2056.

Fink, S.P., Mikkola, D., Willson, J.K., and Markowitz, S. (2003). TGF-b-induced nuclear localization of Smad2 and Smad3 in Smad4 null cancer cell lines. Oncogene *22*, 1317–1323.

Guan, T., Dominguez, C.X., Amezquita, R.A., Laidlaw, B.J., Cheng, J., Henao-Mejia, J., Williams, A., Flavell, R.A., Lu, J., and Kaech, S.M. (2018). ZEB1, ZEB2, and the miR-200 family form a counterregulatory network to regulate CD8+ T cell fates. Journal of Experimental Medicine *215*, 1153–1168.

Herndler-Brandstetter, D., Ishigame, H., Shinnakasu, R., Plajer, V., Stecher, C., Zhao, J., Lietzenmayer, M., Kroehling, L., Takumi, A., Kometani, K., et al. (2018). KLRG1+ Effector CD8+ T Cells Lose KLRG1, Differentiate into All Memory T Cell Lineages, and Convey Enhanced Protective Immunity. Immunity *48*, 716-729.e8.

Hogquist, K.A., Jameson, S.C., Heath, W.R., Howard, J.L., Bevan, M.J., and Carbone, F.R. (1994). T cell receptor antagonist peptides induce positive selection. Cell *76*, 17–27.

Hu, Y., Lee, Y.-T., Kaech, S.M., Garvy, B., and Cauley, L.S. (2015). Smad4 Promotes Differentiation of Effector and Circulating Memory CD8 T Cells but Is Dispensable for Tissue-Resident Memory CD8 T Cells. J Immunol *194*, 2407–2414.

Intlekofer, A.M., Takemoto, N., Wherry, E.J., Longworth, S.A., Northrup, J.T., Palanivel, V.R., Mullen, A.C., Gasink, C.R., Kaech, S.M., Miller, J.D., et al. (2005). Effector and memory CD8+ T cell fate coupled by T-bet and eomesodermin. Nat Immunol *6*, 1236–1244.

Ito, M., Maruyama, T., Saito, N., Koganei, S., Yamamoto, K., and Matsumoto, N. (2006). Killer cell lectin-like receptor G1 binds three members of the classical cadherin family to inhibit NK cell cytotoxicity. Journal of Experimental Medicine *203*, 289–295.

Ji, Y., Pos, Z., Rao, M., Klebanoff, C.A., Yu, Z., Sukumar, M., Reger, R.N., Palmer, D.C., Borman, Z.A., Muranski, P., et al. (2011). Repression of the DNA-binding inhibitor Id3 by Blimp-1 limits the formation of memory CD8+ T cells. Nat Immunol *12*, 1230–1237.

Joshi, N.S., Cui, W., Chandele, A., Lee, H.K., Urso, D.R., Hagman, J., Gapin, L., and Kaech, S.M. (2007). Inflammation Directs Memory Precursor and Short-Lived Effector CD8+ T Cell Fates via the Graded Expression of T-bet Transcription Factor. Immunity *27*, 281–295.

Karecla, P.I., Bowden, S.J., Green, S.J., and Kilshaw, P.J. (1995). Recognition of E-cadherin on epithelial cells by the mucosal T cell integrin αM290β7 (αEβ7). Eur. J. Immunol. *25*, 852–856.

Laidlaw, B.J., Zhang, N., Marshall, H.D., Staron, M.M., Guan, T., Hu, Y., Cauley, L.S., Craft, J., and Kaech, S.M. (2014). CD4+ T Cell Help Guides Formation of CD103+ Lung-Resident Memory CD8+ T Cells during Influenza Viral Infection. Immunity *41*, 633–645.

Lefebvre, M.N., Surette, F.A., Anthony, S.M., Vijay, R., Jensen, I.J., Pewe, L.L., Hancox, L.S., Van Braeckel-Budimir, N., van de Wall, S., Urban, S.L., et al. (2021). Expeditious recruitment of circulating memory CD8 T cells to the liver facilitates control of malaria. Cell Reports *37*, 109956.

Levy, L., and Hill, C.S. (2005). Smad4 Dependency Defines Two Classes of Transforming Growth Factor (TGF-β) Target Genes and Distinguishes TGF-β Induced Epithelial-Mesenchymal Transition from Its Antiproliferative and Migratory Responses. MOL. CELL. BIOL. *25*, 8108–8125.

Mackay, L.K., Wynne-Jones, E., Freestone, D., Pellicci, D.G., Mielke, L.A., Newman, D.M., Braun, A., Masson, F., Kallies, A., Belz, G.T., et al. (2015). T-box Transcription Factors Combine with the Cytokines TGF-β and IL-15 to Control Tissue-Resident Memory T Cell Fate. Immunity *43*, 1101–1111.

Mackay, L.K., Minnich, M., Kragten, N.A.M., Liao, Y., Nota, B., Seillet, C., Zaid, A., Man, K., Preston, S., Freestone, D., et al. (2016). Hobit and Blimp1 instruct a universal transcriptional program of tissue residency in lymphocytes. Science *352*, 459–463.

Malhotra, N., Robertson, E., and Kang, J. (2010). SMAD2 Is Essential for TGFβ-mediated Th17 Cell Generation*. Journal of Biological Chemistry *285*, 29044–29048.

Mani, V., Bromley, S.K., Äijö, T., Mora-Buch, R., Carrizosa, E., Warner, R.D., Hamze, M., Sen, D.R., Chasse, A.Y., Lorant, A., et al. (2019). Migratory DCs activate TGF-β to precondition naïve $CD8^+$ T cells for tissue-resident memory fate. Science *366*, eaav5728.

Massagué, J. (2012). TGFβ signalling in context. Nat Rev Mol Cell Biol *13*, 616–630.

McLane, L.M., Banerjee, P.P., Cosma, G.L., Makedonas, G., Wherry, E.J., Orange, J.S., and Betts, M.R. (2013). Differential Localization of T-bet and Eomes in CD8 T Cell Memory Populations. J.I. *190*, 3207–3215.

Milner, J.J., Toma, C., Yu, B., Zhang, K., Omilusik, K., Phan, A.T., Wang, D., Getzler, A.J., Nguyen, T., Crotty, S., et al. (2017). Runx3 programs CD8+ T cell residency in non-lymphoid tissues and tumours. Nature *552*, 253–257.

Mionnet, C., Sanos, S.L., Mondor, I., Jorquera, A., Laugier, J.-P., Germain, R.N., and Bajénoff, M. (2011). High endothelial venules as traffic control points maintaining lymphocyte population homeostasis in lymph nodes. Blood *118*, 6115–6122.

Mueller, S.N., Gebhardt, T., Carbone, F.R., and Heath, W.R. (2013). Memory T Cell Subsets, Migration Patterns, and Tissue Residence. Annu. Rev. Immunol. *31*, 137–161.

Nath, A.P., Braun, A., Ritchie, S.C., Carbone, F.R., Mackay, L.K., Gebhardt, T., and Inouye, M. (2019). Comparative analysis reveals a role for TGF-β in shaping the residency-related transcriptional signature in tissue-resident memory CD8+ T cells. PLoS ONE *14*, e0210495.

Obar, J.J., Jellison, E.R., Sheridan, B.S., Blair, D.A., Pham, Q.-M., Zickovich, J.M., and Lefrançois, L. (2011). Pathogen-Induced Inflammatory Environment Controls Effector and Memory CD8 $^{+}$ T Cell Differentiation. J.I. *187*, 4967–4978.

Omilusik, K.D., Nadjsombati, M.S., Shaw, L.A., Yu, B., Milner, J.J., and Goldrath, A.W. (2018). Sustained Id2 regulation of E proteins is required for terminal differentiation of effector CD8+ T cells. Journal of Experimental Medicine *215*, 773–783.

Parga-Vidal, L., Behr, F.M., Kragten, N.A.M., Nota, B., Wesselink, T.H., Kavazović, I., Covill, L.E., Schuller, M.B.P., Bryceson, Y.T., Wensveen, F.M., et al. (2021). Hobit identifies tissue-resident memory T cell precursors that are regulated by Eomes. Sci. Immunol. *6*, eabg3533.

Pearce, E.L., Mullen, A.C., Martins, G.A., Krawczyk, C.M., Hutchins, A.S., Zediak, V.P., Banica, M., DiCioccio, C.B., Gross, D.A., Mao, C.-A., et al. (2003). Control of Effector CD8+ T Cell Function by the Transcription Factor Eomesodermin. Science *302*, 1041–1043.

Pope, C., Kim, S.-K., Marzo, A., Williams, K., Jiang, J., Shen, H., and Lefrançois, L. (2001). Organ-Specific Regulation of the CD8 T Cell Response to *Listeria monocytogenes* Infection. J Immunol *166*, 3402–3409.

Sallusto, F., Lenig, D., and Lanzavecchia, A. (1999). Two subsets of memory T lymphocytes with distinct homing potentials and effector functions. *401*, 5.

Sanjabi, S., Mosaheb, M.M., and Flavell, R.A. (2009). Opposing Effects of TGF-β and IL-15 Cytokines Control the Number of Short-Lived Effector CD8+ T Cells. Immunity *31*, 131–144.

Schultz-Cherry, S., and Hinshaw, V.S. (1996). Influenza virus neuraminidase activates latent transforming growth factor beta. J Virol *70*, 8624–8629.

Skon, C.N., Lee, J.-Y., Anderson, K.G., Masopust, D., Hogquist, K.A., and Jameson, S.C. (2013). Transcriptional downregulation of S1pr1 is required for the establishment of resident memory CD8+ T cells. Nat Immunol *14*, 1285–1293.

Suarez-Ramirez, J.E., Chandiran, K., Brocke, S., and Cauley, L.S. (2019). Immunity to Respiratory Infection Is Reinforced Through Early Proliferation of Lymphoid TRM Cells and Prompt Arrival of Effector CD8 T Cells in the Lungs. Front. Immunol. *10*, 1370.

Subramanian, A., Tamayo, P., Mootha, V.K., Mukherjee, S., Ebert, B.L., Gillette, M.A., Paulovich, A., Pomeroy, S.L., Golub, T.R., Lander, E.S., et al. (2005). Gene set enrichment analysis: A knowledge-based approach for interpreting genome-wide expression profiles. Proceedings of the National Academy of Sciences *102*, 15545–15550.

Sun, Y., Liu, X., Ng-Eaton, E., Lodish, H.F., and Weinberg, R.A. (1999). SnoN and Ski protooncoproteins are rapidly degraded in response to transforming growth factor signaling. *96*, 12442–12447.

Takimoto, T., Wakabayashi, Y., Sekiya, T., Inoue, N., Morita, R., Ichiyama, K., Takahashi, R., Asakawa, M., Muto, G., Mori, T., et al. (2010). Smad2 and Smad3 Are Redundantly Essential for the TGF-β–Mediated Regulation of Regulatory T Plasticity and Th1 Development. J Immunol *185*, 842–855.

Teraki, Y., and Shiohara, T. (2002). Preferential expression of aEb7 integrin (CD103) on CD8+ T cells in the psoriatic epidermis: regulation by interleukins 4 and 12 and transforming growth factor-b. British Journal of Dermatology 9.

Tessmer, M.S., Fugere, C., Stevenaert, F., Naidenko, O.V., Chong, H.J., Leclercq, G., and Brossay, L. (2007). KLRG1 binds cadherins and preferentially associates with SHIP-1. International Immunology *19*, 391–400.

Wakim, L.M., Woodward-Davis, A., Liu, R., Hu, Y., Villadangos, J., Smyth, G., and Bevan, M.J. (2012). The Molecular Signature of Tissue Resident Memory CD8 T Cells Isolated from the Brain. J.I. *189*, 3462–3471.

Wang, A., Pan, D., Lee, Y.-H., Martinez, G.J., Feng, X., and Dong, C. (2013). Cutting Edge: Smad2 and Smad4 Regulate TGF-β–Mediated *Il9* Gene Expression via EZH2 Displacement. J.I. *191*, 4908–4912.

Wu, B., Zhang, G., Guo, Z., Wang, G., Xu, X., Li, J., Whitmire, J.K., Zheng, J., and Wan, Y.Y. (2020). The SKI proto-oncogene restrains the resident CD103+CD8+ T cell response in viral clearance. Cell Mol Immunol.

Wu, T., Hu, Y., Lee, Y.-T., Bouchard, K.R., Benechet, A., Khanna, K., and Cauley, L.S. (2014). Lung-resident memory CD8 T cells ($T_{RM}$) are indispensable for optimal cross-protection against pulmonary virus infection. Journal of Leukocyte Biology *95*, 215–224.

Yagi, K., Goto, D., Hamamoto, T., Takenoshita, S., Kato, M., and Miyazono, K. (1999). Alternatively Spliced Variant of Smad2 Lacking Exon 3. Journal of Biological Chemistry *274*, 703–709.

Yang, C.Y., Best, J.A., Knell, J., Yang, E., Sheridan, A.D., Jesionek, A.K., Li, H.S., Rivera, R.R., Lind, K.C., D'Cruz, L.M., et al. (2011). The transcriptional regulators Id2 and Id3 control the formation of distinct memory CD8+ T cell subsets. Nat Immunol *12*, 1221–1229.

Zhang, N., and Bevan, M.J. (2013). Transforming Growth Factor-β Signaling Controls the Formation and Maintenance of Gut-Resident Memory T Cells by Regulating Migration and Retention. Immunity *39*, 687–696.

Zhu, Y., Ju, S., Chen, E., Dai, S., Li, C., Morel, P., Liu, L., Zhang, X., and Lu, B. (2010). T-bet and Eomesodermin Are Required for T Cell-Mediated Antitumor Immune Responses. J.I. *185*, 3174–3183.

**Acknowledgments:** Cells were purified with the assistance of the Flow cytometry Core Facility at UCONN Health. This work was funded by NIH grant AI123864 (LSC and SK).

**Author Contributions**:

Conceptualization and investigation: K.C., J.S-R., Y.H., J.S.L., and Z.U. Formal analysis: B.M. Writing – Original Draft: K.C and L.S.C. Writing – Review & Editing: J.S-R., J.S-L., B.M., and S.K. Funding Acquisition: L.S.C. and S.K. Project administration: L.S.C. and S.K.

**Declaration of Interests:**

The authors have no conflict of interests.

## Figure legends.

**Graphical abstract:** *TGF$\beta$ and SMAD4 modulate gene expression in reciprocal directions during differentiation of antiviral CTLs.*

**Figure 1.** *SMAD4-ablation alters homing receptor expression without TGF$\beta$ receptor II*.

OTI-Ctrl, OTI-TR2KO, OTI-S4KO and OTI-S4TR2-DKO cells were transferred to C57BL/6 mice before infection with X31-OVA. On the days shown, CD45.1$^+$ cells in the lungs and spleens were analyzed by flow cytometry.

**A).** The heatmap shows percentages of donor cells that expressed KLRG1, CD103, CD62L and CD127. Data are means $\pm$SD (n=3/group). Two independent experiments gave similar results.

**B).** Histograms show representative CD103 expression on OTI-S4KO (Top panels - dashed lines) and OTI-S4TR2-DKO (lower panels-dotted lines) cells, compared with the respective Cre-deficient controls (grey shading).

**Figure 2.** *The transcriptional profile of SMAD4-deficient CTLs resembles a $T_{RM}$ phenotype*.

**A-C)** Naïve donor cells were transferred to C57BL/6 mice before infection with X31-OVA. Early effector (EE) cells were analyzed 6dpi, using RNA isolated from pools of three spleens. Each sample was analyzed in triplicate (Total n=9/group). Genes were ranked according differential expression in S4KO and S4Ctrl cells.

**A).** Heat maps show consistent differences between the transcriptional profiles of OTI-S4Ctrl and OTI-S4KO cells.

**B)**. *Eomes* and *Sell* genes were expressed at reduced levels in OTI-S4KO cells, while *Itgae* was induced.

**C&D).** Gene set enrichment analysis was used to compare the transcriptional profile of OTI-S4KO cells with published data sets derived from IEL 7dpi (GSE107395), IEL30dpi, Liver $T_{RM}$, $T_{EM}$ and

$T_{CM}$ (GSE70813), Brain $T_{RM}$ (GSE39152) and CD8 T cells that were activated *in vitro* in the presence and absence of TGFβ (GSE125471).

**E).** S4Ctrl and S4KO cells were activated *in vitro* with αCD3 and αCD28 for 48hrs and then stimulated with rIL-2 (20U/ml) for additional 48 hours. RNA was extracted for qPCR analysis. Samples were analyzed in triplicate. Graphs show *hobit* expression in S4Ctrl (left) and S4KO (right) cells cultured with DMSO (Filled bars), or SB431542 (10μM) (open bars). Data are relative gene expression (mean ± SD), compared to S4Ctrl cells analyzed 48hrs after TcR stimulation. Two independent experiments gave similar results.

**F&G).** OTI-S4KO, OTI-S4Ctrl, OTI-STKO and OTI-STCtrl cells were transferred to C57BL/6 mice before infection with X31-OVA. On the days shown, CD45.1$^+$ cells in the lungs and spleens were analyzed by flow cytometry. Data are mean ± SD (n=4/group). Two independent experiments gave similar results.

**F).** Eomes expression (MFI) in OTI-S4KO (black fill) and OTI-TR2KO (Cross hatch) cells, with the respective Cre-deficient controls (grey shading).

**G).** T-bet expression (MFI) in OTI-S4KO (black fill) and OTI-TR2KO (Cross hatch) cells, with the respective Cre-deficient controls (grey shading).

**H-J).** OTI-S4Ctrl and OTI-S4KO were transferred to C57BL/6 mice before infection with X31-OVA. Donor cells in the lungs were analyzed for EOMES expression at 8 dpi using imaging flow cytometry. Similarity scores were determined using IDEAS software. Higher similarity scores indicate that some EOMES has translocated into the nucleus.

**H).** Representative staining for EOMES (yellow) and 7-AAD (red) to identify the nuclei.

**I)**. Overlaid histograms show EOMES intensity and similarity scores for OTI-S4Ctrl (grey line) and OTI-S4KO (dashed line) cells.

**J).** Bar graphs show statistical comparisons (means ± SD, n=3) between OTI-S4Ctrl (grey shading) and OTI-S4KO (black fill) cells.

**Figure 3.** *SMAD4 is a positive-regulator of EOMES*.

**A&B)** S4Ctrl and S4KO cells were activated *in vitro* for 48hrs and stimulated with rIL-2 alone (20u/ml), or rIL-2 (20u/ml) plus TGFβ (10ng/ml). At 24hrs and 48hrs after cytokine stimulation, RNA was extracted for qPCR analysis. Samples were analyzed in triplicate. Graphs show relative gene expression (mean ± SD), compared to S4Ctrl cells analyzed 48hrs after TcR stimulation. Two independent experiments gave similar results.

**A).** *Itga*e expression in S4Ctrl (left) and S4KO (right) cells analyzed for 48hrs after stimulation with rIL-2 alone (Filled bars), or rIL-2 plus TGFβ (hatched bars).

**B).** *Eomes* expression in S4Ctrl (left) and S4KO (right) cells analyzed for 48hrs after stimulation with rIL-2 alone (Filled bars), or rIL-2 plus TGFβ (hatched bars).

**C).** S2KO, S3KO, S23-DKO, TR2KO, S4KO, S34-DKO and S4TR2-DKO cells (plus the respective Cre-deficient controls) were activated *in vitro.* After 48hrs, CTLs were stimulated with rIL-2 alone (Filled bars), or rIL-2 plus TGFβ (hatched bars). Samples were analyzed in triplicate. Bars show percentages of cells expressing CD103 (means ±SD). Two independent experiments gave similar results.

**D&E).** OTI-S4Ctrl and OTI-S4KO were transferred to C57BL/6 mice before infection with X31-OVA. At 8 dpi, donor cells in the lungs were analyzed for SMAD2/3 and 7-AAD staining by imaging flow cytometry. Similarity scores were determined using IDEAS software.

**D).** Overlaid histograms show SMAD2/3 and nuclear stain in OTI-S4Ctrl (grey line and OTI-S4KO (dashed line) cells.

**E).** Bar graphs show statistical comparisons (means ± SD, n=3) between similarly scores for OTI-S4Ctrl (grey shading) and OTI-S4KO (black fill) cells.

**Figure 4**. *SMAD4 regulates the Itgae gene via direct and indirect mechanisms*.

**A).** S4KO, EKO and ES4KO cells (plus respective Cre-deficient controls) were activated *in vitro*. Selected wells were supplemented with rIL-2 (20u/ml), or rIL-2 plus SB431542 (10μM). After 48hrs,

CTLs were transferred to new wells for secondary cytokine stimulation. Bars graphs show CD103 expression at 48hrs after stimulation with rIL-2 alone (no fill); rIL-2 plus SB431542 (grey fill) and rIL-2 plus TGFβ (hatched). Data are means ± SD (3 mice per group). P values were calculated using Student T tests. Two independent experiments produced similar results.

**B-E).** Naïve CD8 T cells were activated with anti-CD3/CD28. After 48hrs, activated CTLs were transduced with a retroviral vector encoding Eomes (Eomes-IRES-GFP), or empty vector control (EV-IRES-GFP). $GFP^+$ cells were analyzed by flow cytometry at 96hrs after TcR stimulation. Two independent experiments produced similar results.

**B)**. Overlaid histograms show EOMES expression (MFI) in EKO cells after transduction with Eomes-IRES-GFP (grey shading), or EV-IRES-GFP (dashed line).

**C)** Overlaid histograms show CD103 expression on S4KO and S4Ctrl cells after transduction with EV-IRES-GFP (grey shading) EOMES-IRES-GFP (dashed lines).

**D)** Contour plots show CD103 expression on $GFP^+$ CTLs

**Figure 5**. *CD62L is transcriptionally-regulated via SMAD4 during memory formation*.

**A)** Naïve CD8 T cells from S4KO, EKO, ES4KO and control mice express CD62L at similar levels.

**B)** OVA-specific CTLs were analyzed with MHCI tetramers at 30dpi with X31-OVA. Contour plots show percentages of CTLs that expressed CD62L and CD103 in the lungs and SLO.

**C)** S4KO and S4Ctrl cells were activated (48hrs) and stimulated with cytokines (48hrs) *in vitro.* RNA was extracted for qPCR analysis at 96hrs after TcR stimulation. Graphs show *Sell* and *KLF2* transcripts after stimulation with rIL-2 alone (filled bars), and rIL-2 plus TGFβ (hatched). Data are mean ± SD, n=3/group. Two experiments gave similar results.

**D)** S4KO, EKO, ES4KO cells (plus Cre-deficient controls) were activated (48hrs) and stimulated with cytokines (48hrs) *in vitro*. Bars graphs show percentages of CTLs that expressed CD62L at 48hrs after stimulation with rIL-2 alone (no fill); rIL-2 plus SB431542 (grey fill) and rIL-2 plus TGFβ

(hatched). Data are means ± SD (3 mice per group). P values were calculated using student's T tests. Two independent experiments produced similar results.

**E)** S4KO and S4Ctrl cells were activated *in vitro* and transduced with a retroviral vector encoding Eomes (Eomes-IRES-GFP), or empty vector control (EV-IRES-GFP). Histograms show $GFP^+$ cells analyzed for CD62L expression at 6 days after TcR stimulation. Contour plots show $GFP^+$ cells analyzed for CD62L and CD103. Two independent experiments produced similar results.

**F)** S2KO, S3KO, S23-DKO, TR2KO, S4KO, S34-DKO and S4TR2-DKO cells (plus the respective Cre-deficient controls) were activated *in vitro.* After 48hrs, CTLs were stimulated with rIL-2 alone (filled bars), or rIL-2 plus TGFβ (hatched bars). Bars show percentages of CTLs that expressed CD62L at 48hrs after cytokine stimulation (means ±SD). Two independent experiments gave similar results.

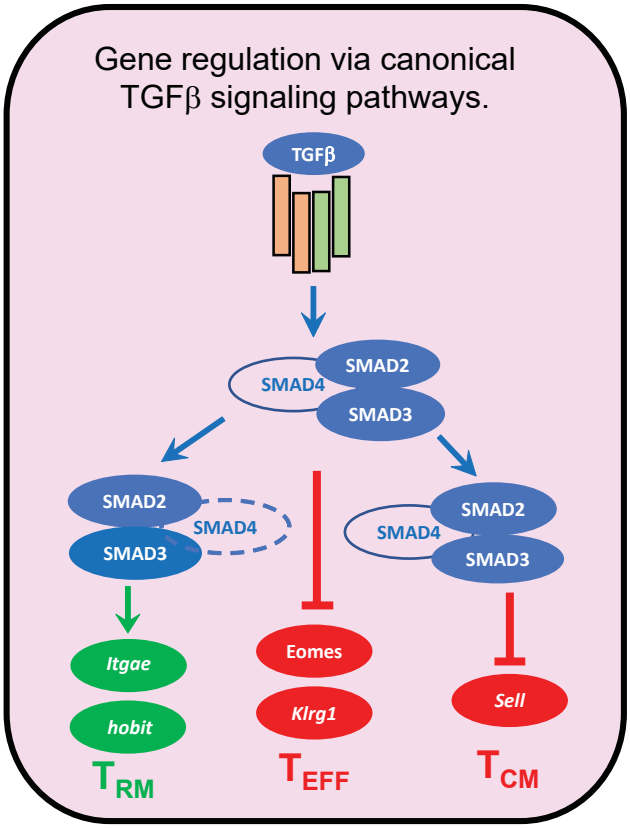
Gene regulation via canonical TGFβ signaling pathways.
TGFβ
SMAD2
SMAD4
SMAD3
SMAD2
SMAD4
SMAD3
SMAD2
SMAD4
SMAD3
Itgae
hobit
Eomes
Klrg1
Sell
TRM
TEFF
TCM

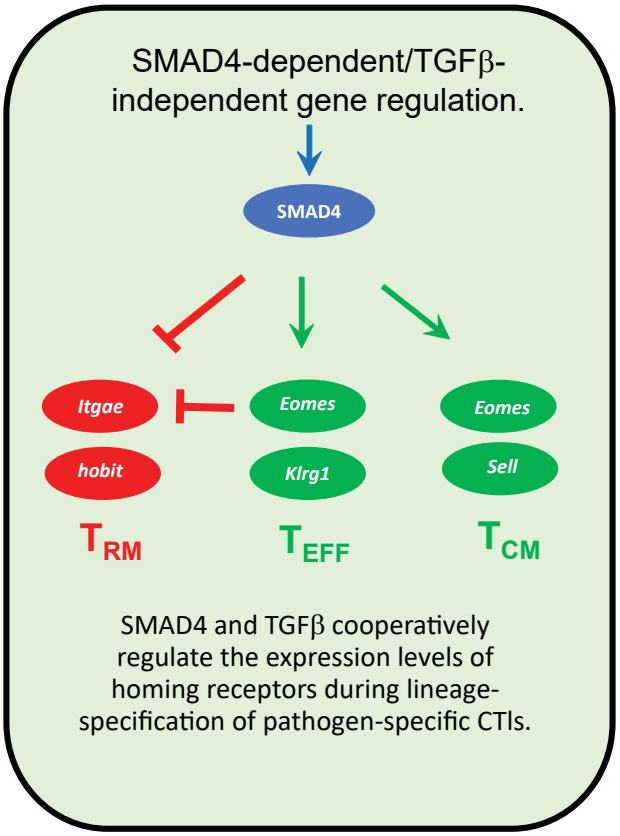
SMAD4-dependent/TGFβ-independent gene regulation.
SMAD4
Itgae
hobit
Eomes
Klrg1
Eomes
Sell
TRM
TEFF
TCM
SMAD4 and TGFβ cooperatively regulate the expression levels of homing receptors during lineage-specification of pathogen-specific CTls.

Figure 1

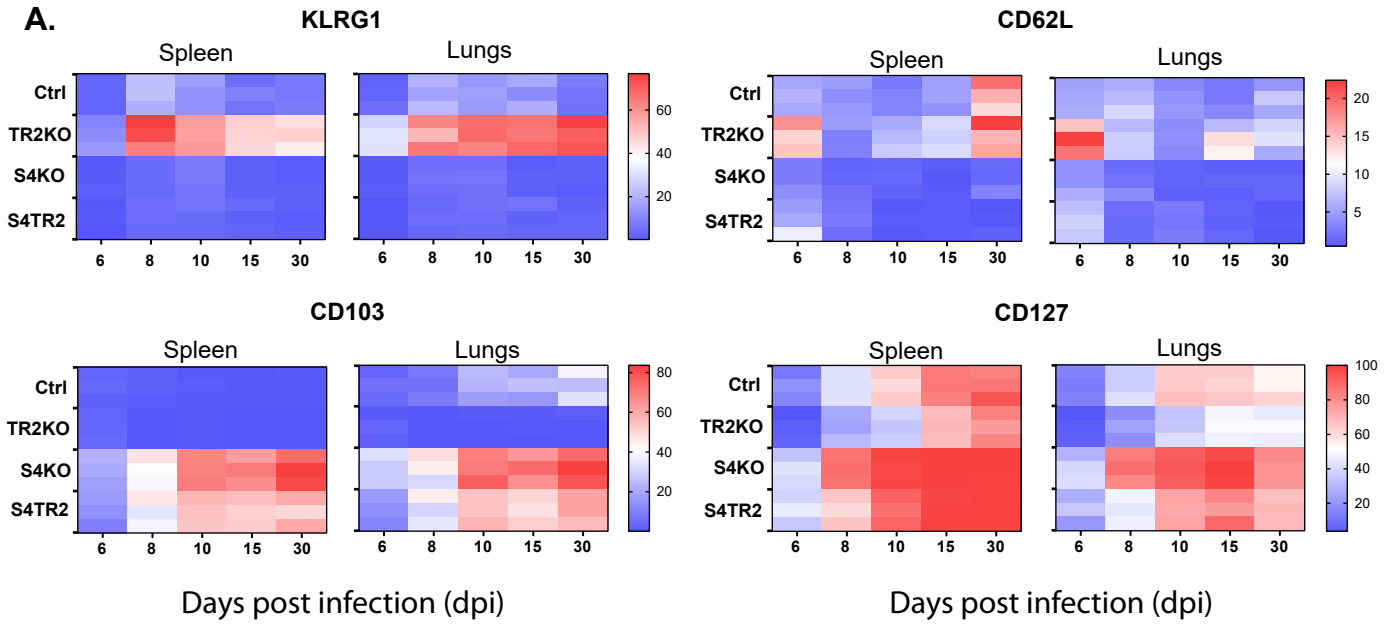
A.
KLRG1
CD62L
CD103
CD127
Spleen
Lungs
Ctrl
TR2KO
S4KO
S4TR2
6
8
10
15
30
Days post infection (dpi)

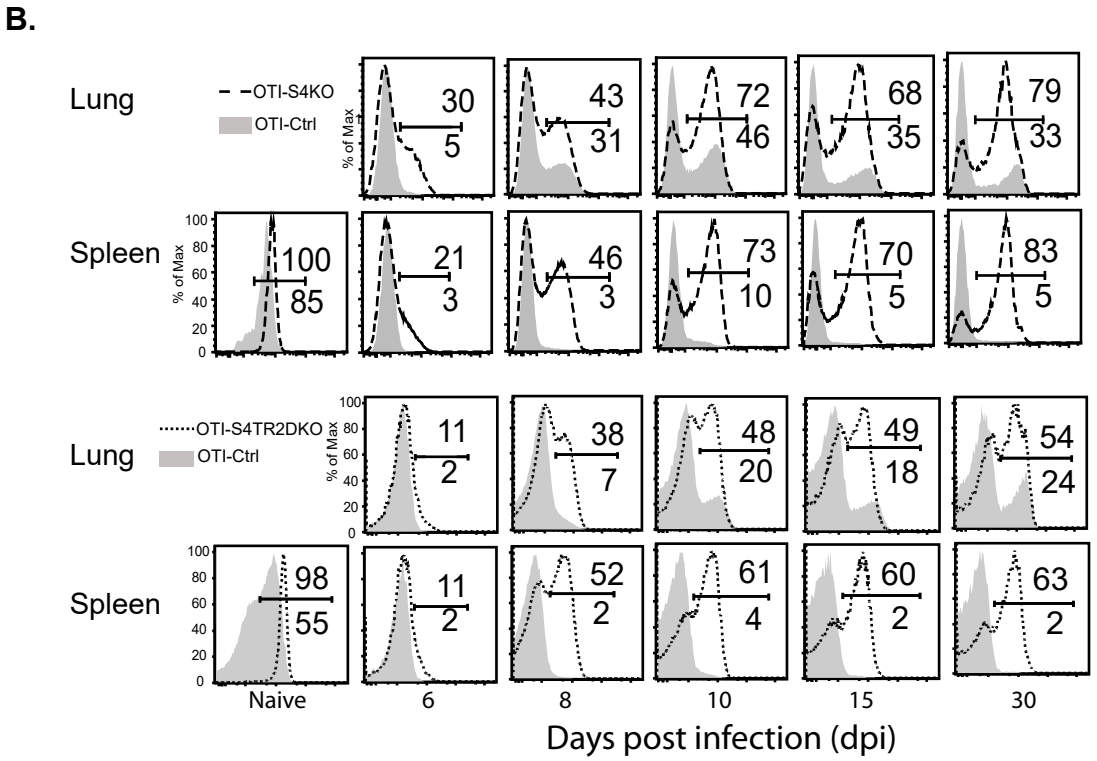
B.
Lung
Spleen
OTI-S4KO
OTI-Ctrl
OTI-S4TR2DKO
% of Max
Naive
6
8
10
15
30
Days post infection (dpi)

Figure 2

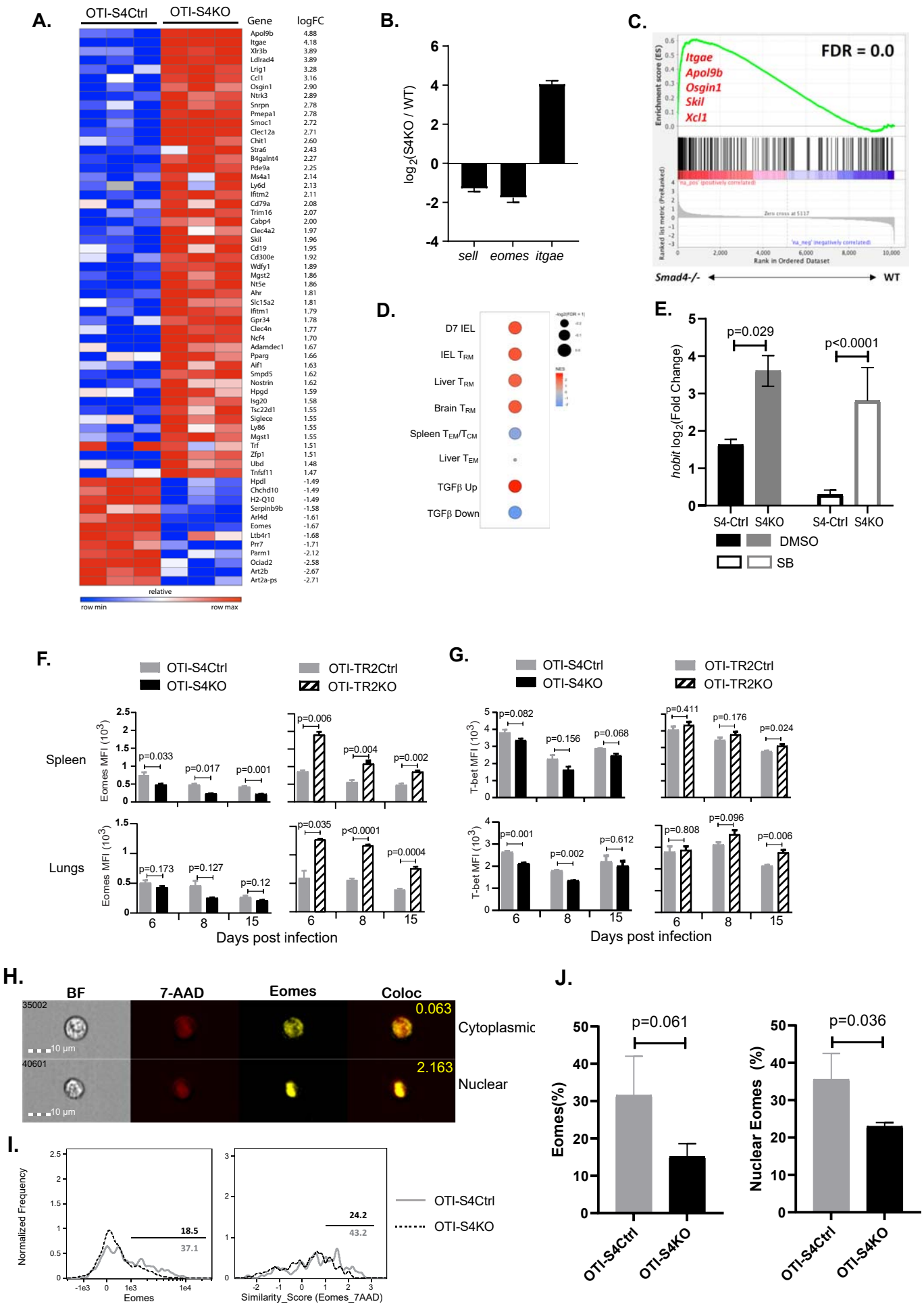
A.
OTI-S4Ctrl
OTI-S4KO
Gene logFC
Apol9b 4.88
Itgae 4.18
Xlr3b 3.89
Ldlrad4 3.89
Lrig1 3.28
Ccl1 3.16
Osgin1 2.90
Ntrk3 2.89
Snrpn 2.78
Pmepa1 2.78
Smoc1 2.72
Clec12a 2.71
Chit1 2.60
Stra6 2.43
B4galnt4 2.27
Pde9a 2.25
Ms4a1 2.14
Ly6d 2.13
Ifitm2 2.11
Cd79a 2.08
Trim16 2.07
Calbp4 2.00
Clec4a2 1.97
Skil 1.96
Cd19 1.95
Cd300e 1.92
Wdfy1 1.89
Mgst2 1.86
Nt5e 1.86
Ahr 1.81
Slc15a2 1.81
Ifitm1 1.79
Gpr34 1.78
Clec4n 1.77
Ncf4 1.70
Adamdec1 1.67
Pparg 1.66
Aif1 1.63
Smpd5 1.62
Nostrin 1.62
Hpgd 1.59
Isg20 1.58
Tsc22d1 1.55
Siglece 1.55
Ly86 1.55
Mgst1 1.55
Trf 1.51
Zfp1 1.51
Ubd 1.48
Tnfsf11 1.47
Hpdl -1.49
Chchd10 -1.49
H2-Q10 -1.49
Serpinb9b -1.58
Arl4d -1.61
Eomes -1.67
Ltb4r1 -1.68
Prr7 -1.71
Parm1 -2.12
Ociad2 -2.58
Art2b -2.67
Art2a-ps -2.71
relative
row min
row max
B.
log2(S4KO / WT)
sell
eomes
itgae
C.
FDR = 0.0
Itgae
Apol9b
Osgin1
Skil
Xcl1
Enrichment score (ES)
Ranked list metric (PreRanked)
Rank in Ordered Dataset
Smad4-/-
WT
D.
D7 IEL
IEL TRM
Liver TRM
Brain TRM
Spleen TEM/TCM
Liver TEM
TGFβ Up
TGFβ Down
E.
hobit log2(Fold Change)
p=0.029
p<0.0001
S4-Ctrl
S4KO
S4-Ctrl
S4KO
DMSO
SB
F.
OTI-S4Ctrl
OTI-S4KO
OTI-TR2Ctrl
OTI-TR2KO
Spleen
Lungs
Eomes MFI (10^3)
p=0.033
p=0.017
p=0.001
p=0.006
p=0.004
p=0.002
p=0.173
p=0.127
p=0.12
p=0.035
p<0.0001
p=0.0004
6
8
15
Days post infection
G.
T-bet MFI (10^3)
p=0.082
p=0.156
p=0.068
p=0.411
p=0.176
p=0.024
p=0.001
p=0.002
p=0.612
p=0.808
p=0.096
p=0.006
Days post infection
H.
BF
7-AAD
Eomes
Coloc
35002
40601
10 µm
0.063
2.163
Cytoplasmic
Nuclear
I.
Normalized Frequency
18.5
37.1
24.2
43.2
Eomes
Similarity_Score (Eomes_7AAD)
OTI-S4Ctrl
OTI-S4KO
J.
Eomes(%)
Nuclear Eomes (%)
p=0.061
p=0.036
OTI-S4Ctrl
OTI-S4KO

Figure 3.

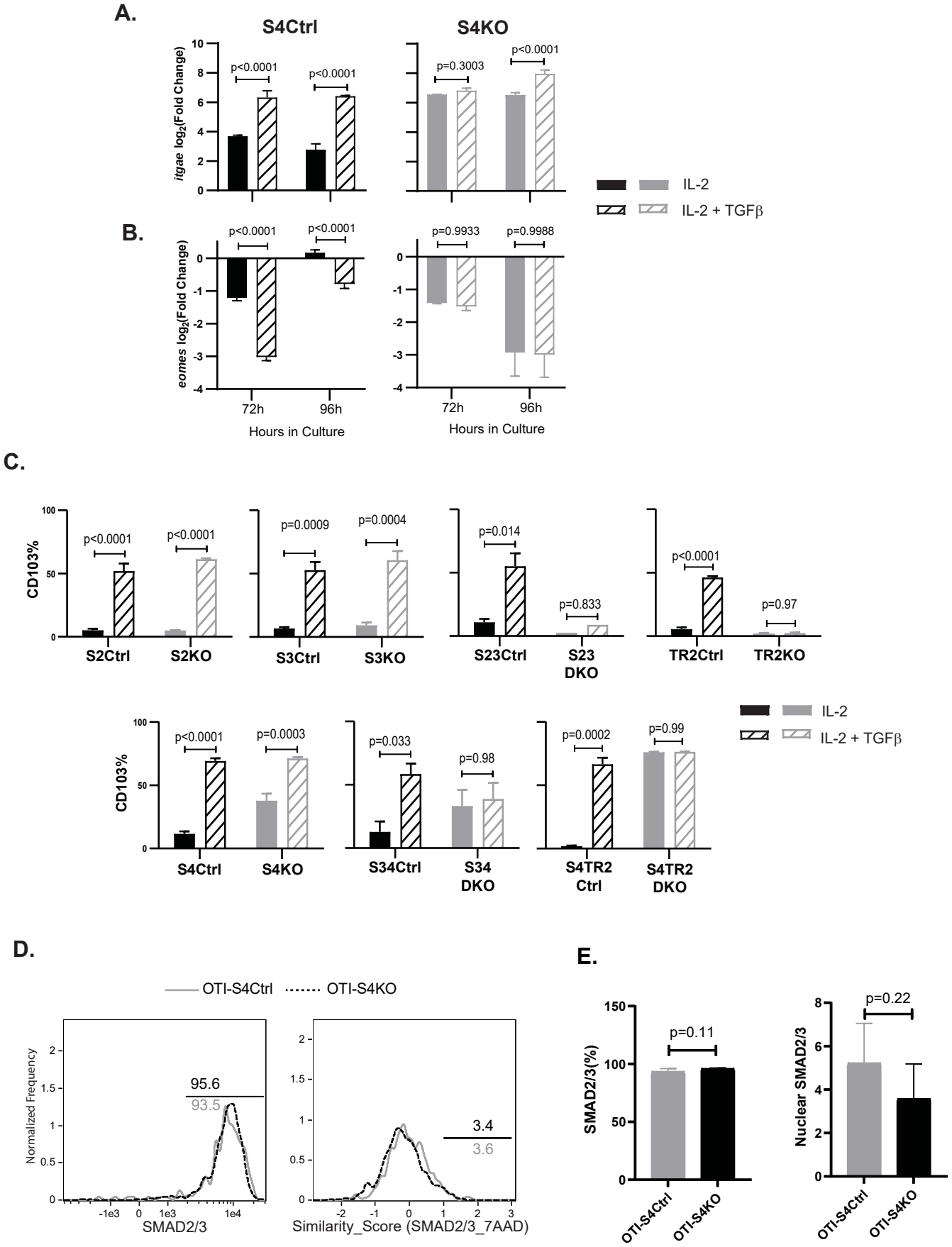
A.
S4Ctrl
S4KO
itgae log2(Fold Change)
p<0.0001
p<0.0001
p=0.3003
p<0.0001
IL-2
IL-2 + TGFβ
B.
eomes log2(Fold Change)
p<0.0001
p<0.0001
p=0.9933
p=0.9988
72h
96h
Hours in Culture
C.
CD103%
p<0.0001
p<0.0001
p=0.0009
p=0.0004
p=0.014
p=0.833
p<0.0001
p=0.97
S2Ctrl
S2KO
S3Ctrl
S3KO
S23Ctrl
S23 DKO
TR2Ctrl
TR2KO
p<0.0001
p=0.0003
p=0.033
p=0.98
p=0.0002
p=0.99
S4Ctrl
S4KO
S34Ctrl
S34 DKO
S4TR2 Ctrl
S4TR2 DKO
D.
OTI-S4Ctrl
OTI-S4KO
Normalized Frequency
95.6
93.5
3.4
3.6
SMAD2/3
Similarity_Score (SMAD2/3_7AAD)
E.
SMAD2/3(%)
p=0.11
Nuclear SMAD2/3
p=0.22
OTI-S4Ctrl
OTI-S4KO

Figure 4.

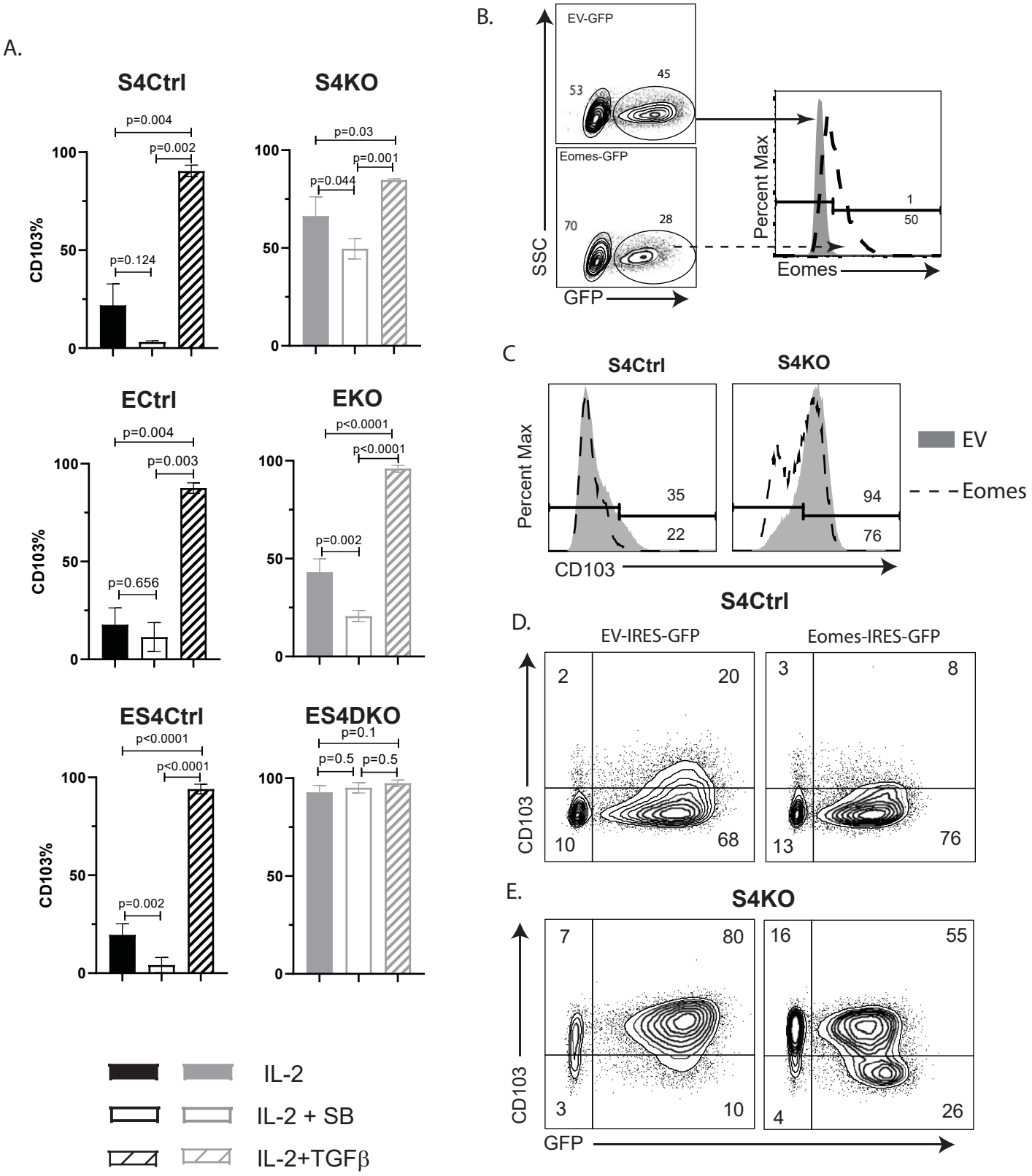
A.
S4Ctrl
S4KO
ECtrl
EKO
ES4Ctrl
ES4DKO
CD103%
p=0.004
p=0.002
p=0.124
p=0.03
p=0.001
p=0.044
p=0.003
p=0.656
p<0.0001
p=0.1
p=0.5
IL-2
IL-2 + SB
IL-2+TGFβ
B.
EV-GFP
Eomes-GFP
SSC
GFP
Percent Max
Eomes
C
S4Ctrl
S4KO
Percent Max
CD103
EV
Eomes
D.
S4Ctrl
EV-IRES-GFP
Eomes-IRES-GFP
CD103
E.
S4KO
CD103
GFP

Figure 5.

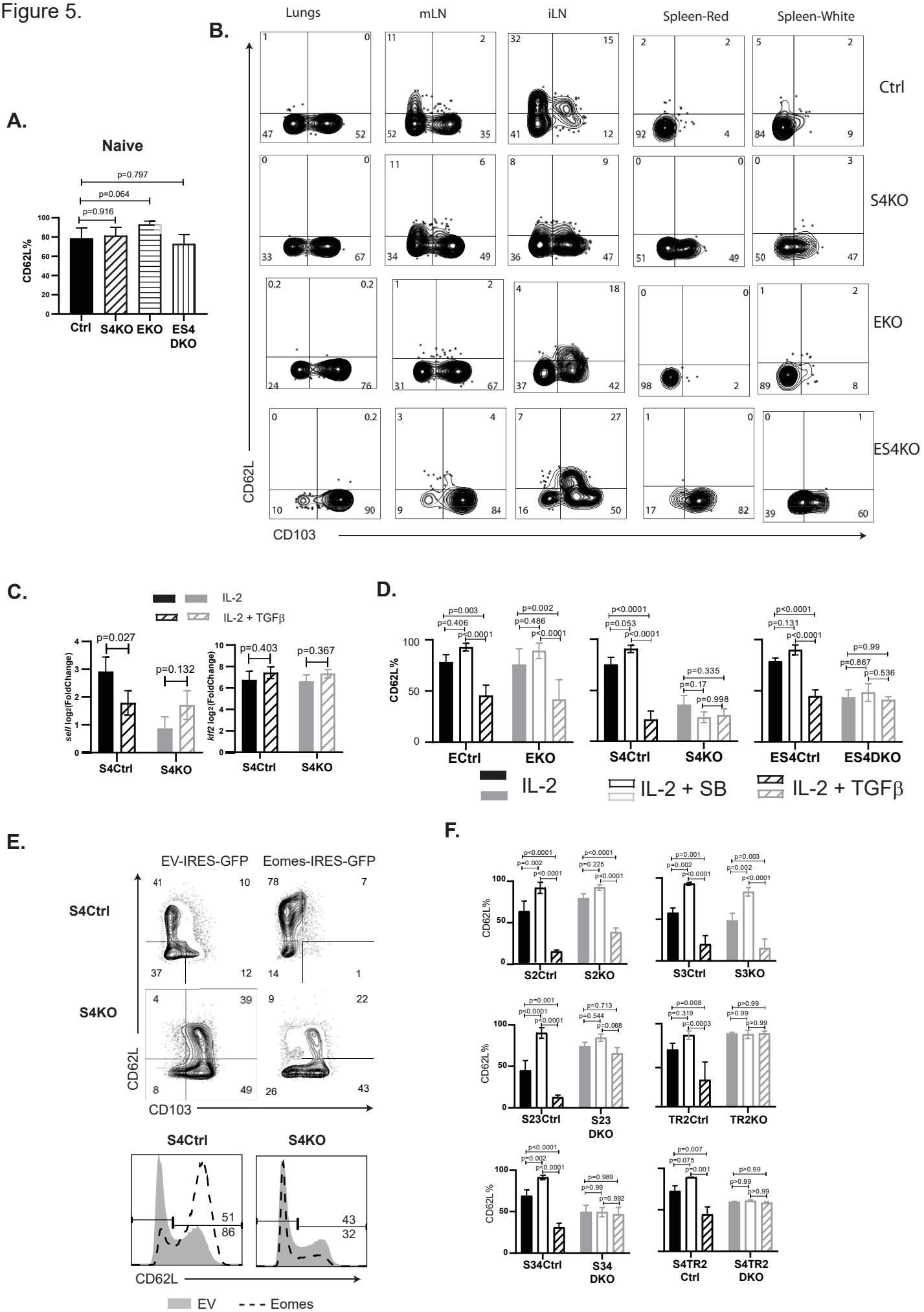
A.
Naive
p=0.797
p=0.064
p=0.916
CD62L%
Ctrl
S4KO
EKO
ES4 DKO
B.
Lungs
mLN
iLN
Spleen-Red
Spleen-White
Ctrl
S4KO
EKO
ES4KO
CD62L
CD103
C.
IL-2
IL-2 + TGFβ
p=0.027
p=0.132
p=0.403
p=0.367
sel/ log2(FoldChange)
klf2 log2(FoldChange)
S4Ctrl
S4KO
D.
p=0.003
p=0.406
p<0.0001
p=0.002
p=0.486
p<0.0001
p<0.0001
p=0.053
p<0.0001
p=0.335
p=0.17
p=0.998
p<0.0001
p=0.131
p<0.0001
p=0.99
p=0.867
p=0.536
CD62L %
ECtrl
EKO
S4Ctrl
S4KO
ES4Ctrl
ES4DKO
IL-2
IL-2 + SB
IL-2 + TGFβ
E.
EV-IRES-GFP
Eomes-IRES-GFP
S4Ctrl
S4KO
CD62L
CD103
51
86
43
32
EV
Eomes
F.
CD62L %
S2Ctrl
S2KO
S3Ctrl
S3KO
S23Ctrl
S23 DKO
TR2Ctrl
TR2KO
S34Ctrl
S34 DKO
S4TR2 Ctrl
S4TR2 DKO

**Supplemental Data.**

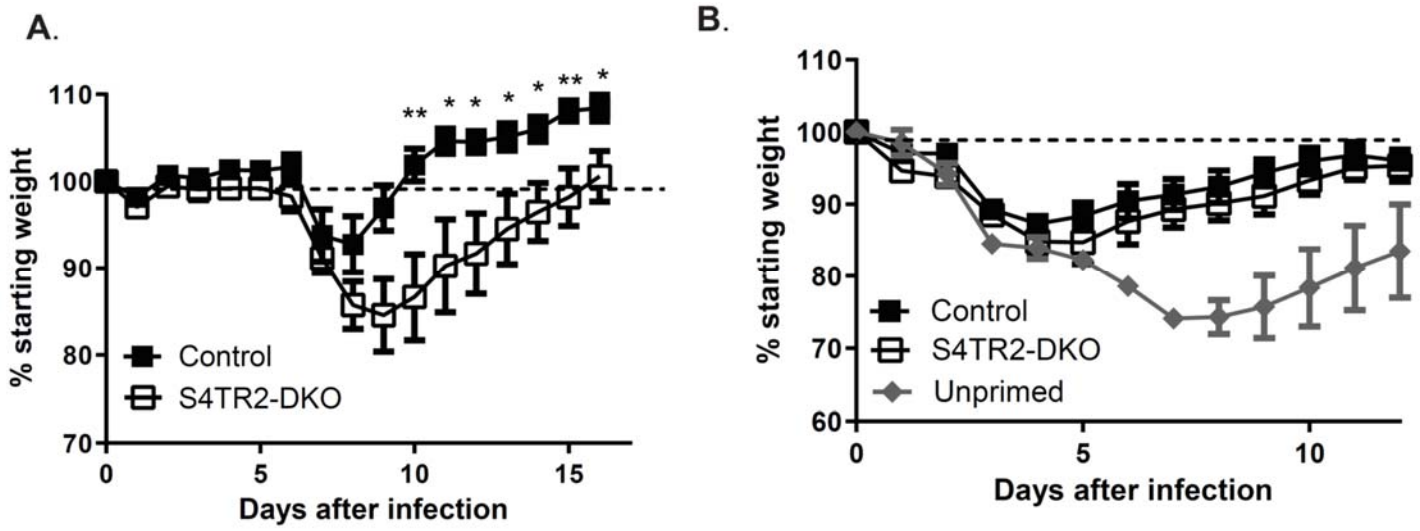


**Figure Supplement 1.** *Weight loss after IAV infection*

Mice were infected with X31-OVA (H3N2 serotype) and weighed daily. At 30dpi, the mice challenged with WSN-OVA$_I$ (H1N1 serotype). Graphs show weight loss as % change from baseline (day 0). Symbols indicate statistical comparisons with controls P<0.05 (*), P<0.01 (**). Combined data from two independent experiments are shown.

**A)** Weight change in S4TR2-Ctrl (filled squares) and S4TR2-DKO mice (open squares) after primary infection with X31-OVA

**B).** Weight change in S4TR2-Ctrl (filled squares) and S4TR2-DKO mice (open squares) after secondary infection with WSN-OVA$_I$. UP are unprimed control mice

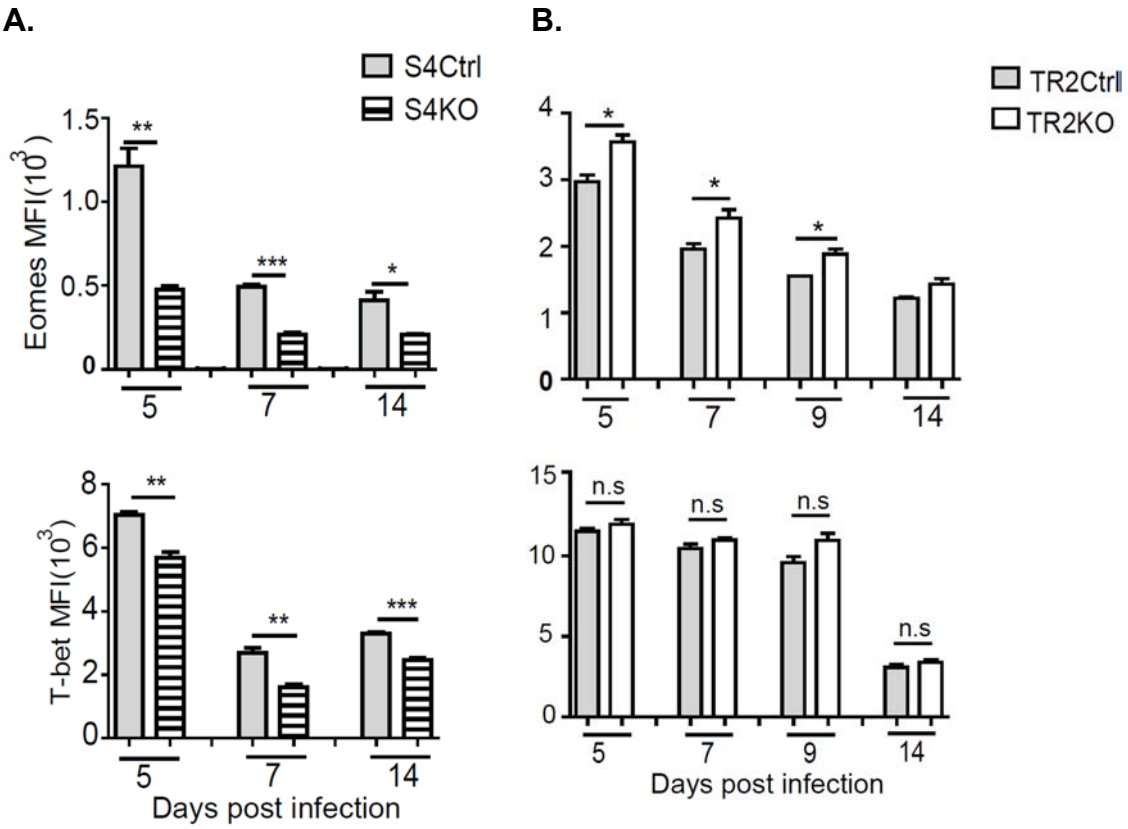


**Figure Supplement 2.** *Tbox transcription factors were analyzed by flow cytometry after infection LM-OVA.*

OTI-S4KO, OTI-S4Ctrl, OTI-TR2KO and OTI-TR2Ctrl cells were transferred to C57BL/6 mice before infection with LM-OVA. On the days shown, CD45.1$^{+}$ cells in the lungs and spleens were analyzed by flow cytometry. Data are mean $\pm$ SD (n=4/group). Two independent experiments gave similar results. P $\geq$ 0.05 (non-significant; ns), P<0.05 (*), P<0.01 (**), P<0.001 (***), P<0.0001 (****).

**A)** Eomes expression (MFI) in OTI-S4KO (black fill) and OTI-TR2KO (Cross hatch) cells, with the respective Cre-deficient controls (grey shading).

**B).** T-bet expression (MFI) in OTI-S4KO (black fill) and OTI-TR2KO (Cross hatch) cells, with the respective Cre-deficient controls (grey shading).

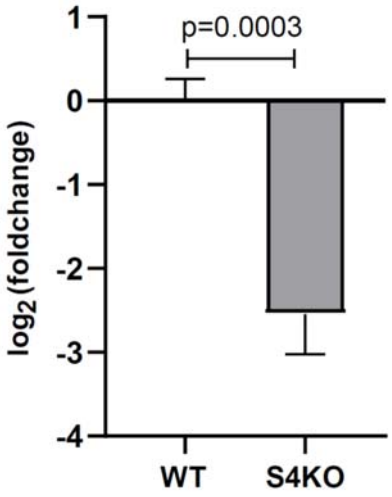


**Figure Supplement 3.** *SMAD4 upregulates Klrg1 expression***.**

OTI-S4KO and OTI-S4Ctrl cells were transferred to C57BL/6 mice before infection with LM-OVA. Donor cells were isolated from the spleens at 8dpi. *Klrg1* transcripts were analyzed by qPCR.

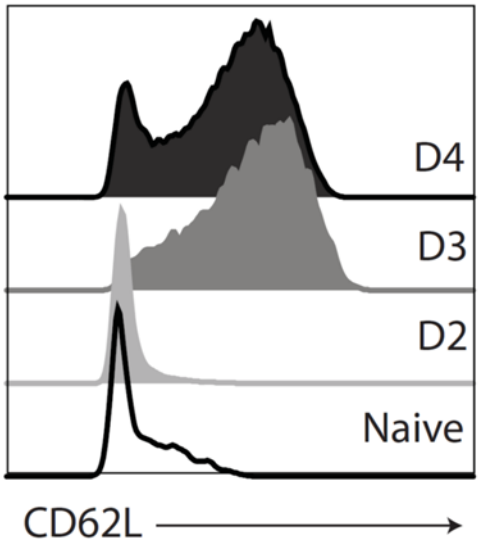


**Figure Supplement 4**: *Changes in CD62L expression on CD8 T cells during TcR stimulation*.

Naïve CD8 T cells were purified from SLO in C57BL/6 mice and stimulated with anti-CD3/CD28 and rIL-2 (48hrs) then washed and cultured with rIL-2 (48hrs) without TcR stimulation. Aliquots of CD8 T cells were analyzed for CD62L expression at the times indicated.